AFCRL-67-0657

ALBERTA HAIL STUDIES 1966

Four contributions by

A. J. Chisholm, Marianne English,
Walter Hitschfeld, J. Pell, N. H. Thyer

McGILL UNIVERSITY
MONTREAL, CANADA

STORMY WEATHER GROUP
SCIENTIFIC REPORT

MW-49

Contract No. F19628-67-C-0129
Project No. 8620
Task No. 862004
Work Unit No. 86200401
Scientific Report No. 2

MAY 1967

This report was prepared with the support of the Canadian Meteorological Service

Contract Monitor: Ralph J. Donaldson
Meteorology Laboratory

Prepared for

Air Force Cambridge Research Laboratories
Office of Aerospace Research
United States Air Force
Bedford, Massachusetts 01730

83

ALBERTA HAIL STUDIES 1966

A.J. Chisholm, et al

McGill University
Montreal, Quebec

May 1967

AFCRL-67-0657

ALBERTA HAIL STUDIES 1966

Four contributions by

A. J. Chisholm, Marianne English,
Walter Hitschfeld, J. Pell, N. H. Thyer

McGILL UNIVERSITY
MONTREAL, CANADA

STORMY WEATHER GROUP
SCIENTIFIC REPORT

MW-49

Contract No. F19628-67-C-0129
Project No. 8620
Task No. 862004
Work Unit No. 86200401
Scientific Report No. 2

MAY 1967

This report was prepared with the support
of the Canadian Meteorological Service

Contract Monitor: Ralph J. Donaldson
Meteorology Laboratory

Prepared for

Air Force Cambridge Research Laboratories
Office of Aerospace Research
United States Air Force
Bedford, Massachusetts 01730

A B S T R A C T S

A NEW METHOD OF DOUBLE THEODOLITE PIBAL EVALUATION

Norman H. Thyer

A new method is presented for evaluating double theodolite pibals, using all four theodolite angles to locate the most likely position of the balloon. The calculation may be done graphically, once a special chart has been compiled, and so straightforward calculations of wind are possible without use of a computer.

CONTINUITY IN HAIL PRODUCTION AND SWATHS

A REVIEW

Jerry Pell

The Wokingham storm study made by Browning and Ludlam postulated a steady-state "supercell" which would generate hail continuously along the storm trajectory. Although such storms may very well exist, or as Browning and Fujita point out, some storms may attain a quasi-steady state for certain portions of their lifetimes, there are documented cases of storms which produce intermittent hailswaths, disrupted by patches of only rain. In particular, we may mention the work of Carte in both Africa and Alberta, and of McBride in Alberta. Closely related to the problem of swath continuity is that of continuity of hailfall at a point. Again, reliable reports have been received from observers who indicate that frequently hail may fall in "bursts", separated by periods of either rain or no precipitation at all.

SMALL SCALE STRUCTURE OF ALBERTA HAILSTORMS

A.J. Chisholm

A study of radar echo maxima in two Alberta hailstorms has shown that the storms consisted of several storm "families", each containing small intense radar echo "cores" or cells. These cells developed preferentially on the right flank of the family, moving across the track of the family at an acute angle to dissipate near the left flank; identifiable lifetimes of the cells were 20-30 minutes. There appeared to be a cycle of development of the cells, which had a considerable effect on the overall storm-family velocity.

PREFACE

In the study of a subject as complex as a hailstorm different approaches are necessary. The present Volume, which contains rather diverse items, illustrates the variety of the aspects we need to consider.

Dr. Thyer's contribution is an attempt to systematize the reduction of the four separate measurements obtained by double-theodolites of a balloon rising in the free atmosphere. Four pieces of information are being measured (elevation and azimuth relative to each theodolite); these must then be combined, while minimizing errors, to the three coordinates of the balloon (longitude, latitude and height). Pure theory? Yes. And yet it's a study that is a necessary prerequisite to a program of stereo-pibal observations of the winds near the storm. Such a program is to be part of our field project.

Mr. Pell's article is a summary of a considerable body of studies of the problem of continuity vs intermittency of hail fall-out on the ground, with overtones regarding the steadiness (or otherwise) of the hail mechanism aloft. The conclusion, strongly specialized to the Alberta experience, is that long-lived storms, with wide-spread hail fall-out exist, but that the mechanism within the storm is probably not truly continuous.

This point is illuminated in a different way by Mr. Chisholm. Though the only radar data available derive from an instrument of low spatial resolution and relatively poor intensity discrimination, Chisholm succeeds in mapping the development, migration and decay of regions of intense echo. The echo features he follows are quite possibly evidence of high-updraft cells in which the hail forms. Detailed correlation between these cells and the hail fall-out pattern at the ground has not been possible so far, but special attention to this problem will be paid in future observations; the availability of improved resolution equipment will be helpful here. We do not know the usefulness of the polarizing facility of the new radar in detail, but are hopeful that it too will go some way in allowing us to spot the hail.

The last item in the Volume, by Mrs. English and the writer, is a brief note, intended to correct errors in results reported two years ago (Report MW-42, 1965). The point is somewhat academic now, but at that time it appeared to Mr. Stauder and me that wet hail could harden appreciably if ejected from the cloud into the dry and cold outside. The fact that this is not the case for the larger stone has a bearing in how we must picture the development of hail: this point has already been suggested by Mrs. English in our Report MW-47; formal correction of the arithmetic is made here.

W.H.

ALBERTA HAIL STUDIES, 1966

Scientific Report MW-49

CONTENTS

A NEW METHOD OF DOUBLE THEODOLITE PIBAL EVALUATION

by

Norman H. Thyer

CONTENTS

A NEW METHOD OF DOUBLE THEODOLITE PIBAL EVALUATION

Norman H. Thyer

ABSTRACT

A new method is presented for evaluating double theodolite pibals, using all four theodolite angles to locate the most likely position of the balloon. The calculation may be done graphically, once a special chart has been compiled, and so straightforward calculations of wind are possible without use of a computer.

1. INTRODUCTION

Pilot balloons for upper wind measurements are sometimes followed by two theodolites to eliminate errors due to variation of rate of rise. This gives four coordinates to determine the balloon's position in 3-dimensional space. Only three of these coordinates need to be used, but it often happens that the theodolite readings are not perfect, and so the position calculated varies according to which three of the four coordinates are chosen. In this case, it is desirable to use all four coordinates to estimate the most likely position of the balloon, and also to indicate whether the uncertainty is small enough to have been caused by limits of instrumental accuracy.

A method which does this has already been described (Thyer, 1962). However, it is prohibitively laborious without the aid of an electronic computer.

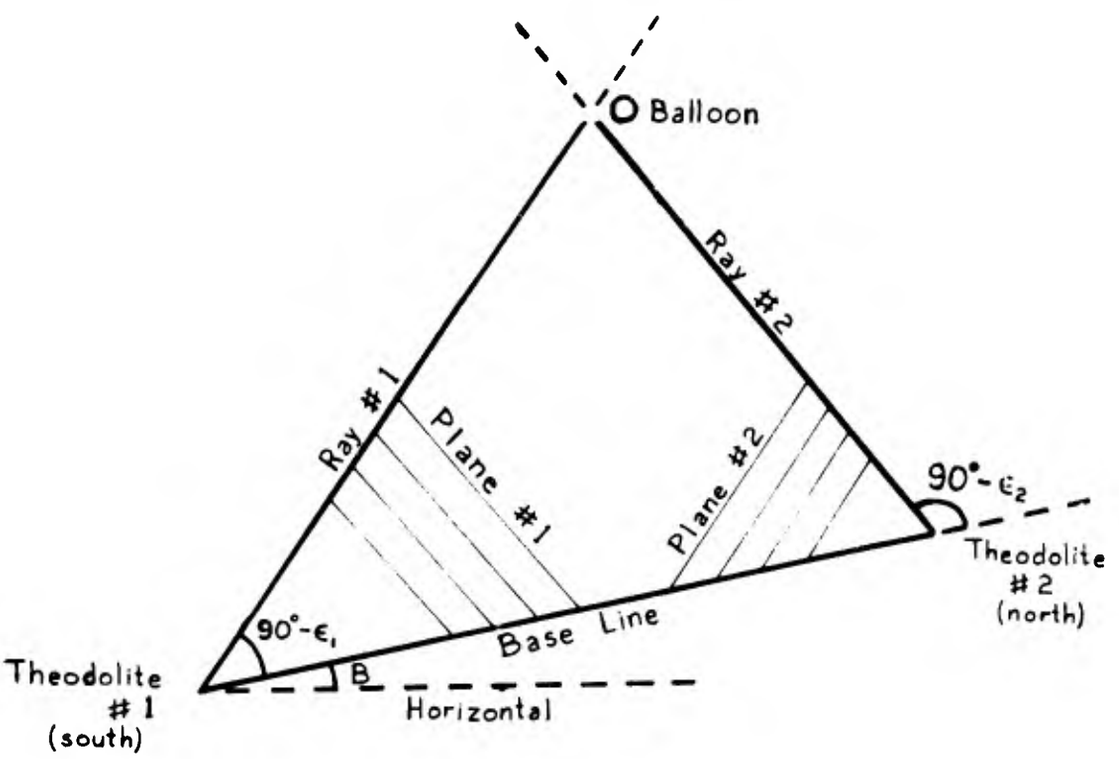

Fig. 1: Positions of theodolites and rays.

2. BASIS OF NEW METHOD

The new method described here also uses all four coordinates, but rather than using vectors, as in the former method, it is based on spherical trigonometry.

For purposes of explanation, we shall assume that theodolite No. 1 is at the south end, and No. 2 at the north end, of the base line, and that azimuths are measured from the north. Usually the theodolites are not at the same elevation. Therefore the baseline itself is not level. Let b be its length, and B the angle it makes with the horizontal, with station No. 2 higher than No. 1. (See Fig. 1).

The angles measured by theodolite No. 1 define a ray passing through the theodolite (Ray No. 1). As the base line also passes through the theodolite, the baseline and the ray define a plane, which we can call Plane No. 1. Similarly the base line and the ray through theodolite No. 2 (Ray No. 2) define another plane which we can call Plane No. 2. If the rays from the two theodolites intersect (or are parallel), the two planes will coincide. Otherwise the planes will not coincide. In the latter case the most probable position of the balloon will be on a plane intermediate between Planes No. 1 and No. 2.

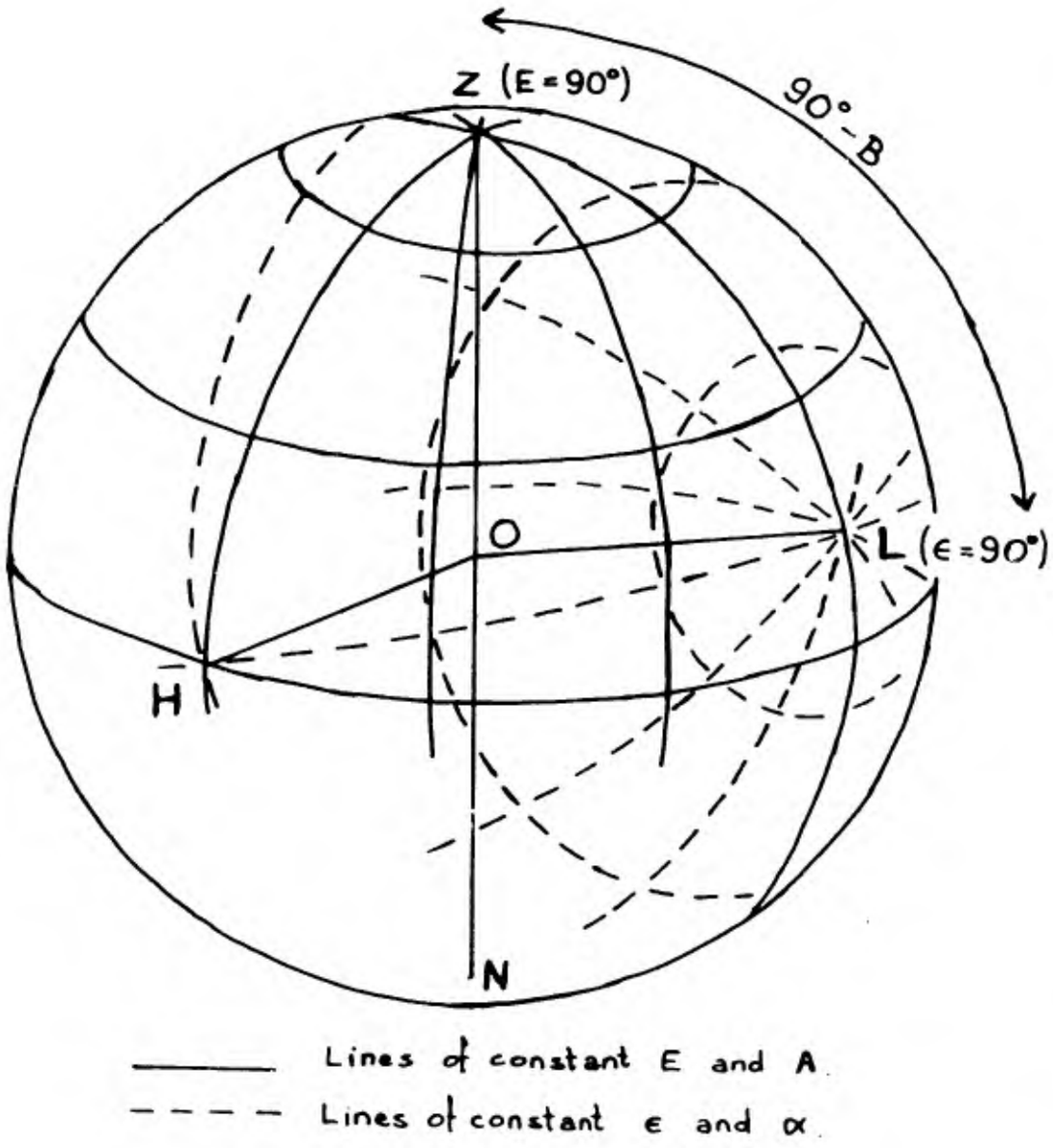

Fig. 2: The two coordinate systems, with poles Z and L, inscribed on a sphere of centre O. Readings are made in the OZ-system, and transformed to the OL-system. OH is perpendicular to both OZ and OL.

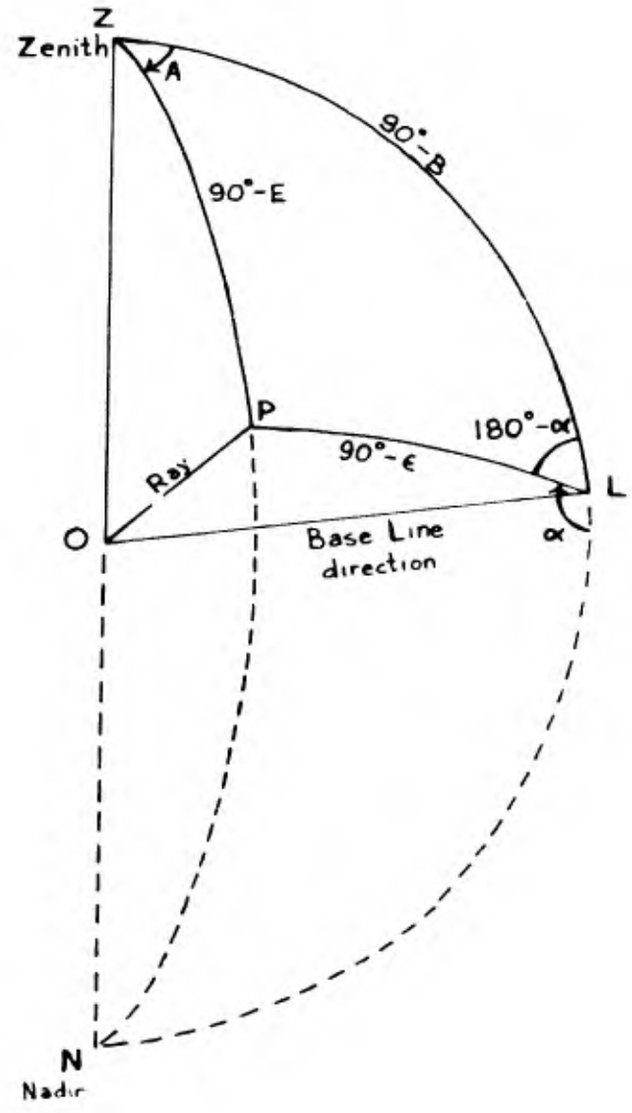

Fig. 3: Spherical Triangle ZPL. OP represents the direction of the balloon, as seen from a theodolite at O. α is angle NLP in spherical triangle NLP. $90^\circ - \epsilon$ is side LP.

3. COORDINATE SYSTEMS

To put this method into workable form, it is useful to introduce a different coordinate system. The original readings taken by each theodolite are in a spherical polar coordinate system whose polar axis is the vertical through the theodolite. A transformation is made to a different spherical polar coordinate system in which the polar axis is the base line joining the two theodolites.

It is helpful to visualize the two coordinate systems as being inscribed on the surface of a sphere of centre O, like the lines of latitude and longitude on a globe. (See Fig. 2) Let Z (the zenith) represent the pole of the system in which the original theodolite readings are made, and in which E represents the elevation, and A the azimuth angle. (I.e. $E = 90^\circ$ at Z.) (See also Fig. 3). Let L be the pole of the new system, in which OL is the direction of the baseline (from south to north), ϵ represents the "latitude" angle and α the "longitude". (I.e. $\epsilon = 90^\circ$ at L.) The angle ZOL is then $90^\circ - B$. The meridian ZL corresponds to $A = 0$, and LN to $\alpha = 0$, N being the nadir. A and α both increase in a clockwise direction as seen from outside the sphere.

In this new coordinate system, at every point in Plane No. 1, α has the same value, which we can call α_1. Also, at every point in Plane No. 2, α has the same value which we can call α_2. Therefore, if the two planes coincide, $\alpha_1 = \alpha_2$, and so by calculating and comparing α_1 and α_2, we can check the accuracy of our fix and also estimate the value of α for the plane in which the balloon probably lies.

For making the transformation into the new system, the relations between the various angles can be found from the spherical triangle ZPL shown in Fig. 3, which represents a perspective looking down on the theodolite at O from the north-east, and in which OP is the direction of the balloon as seen from O. We want to find ϵ and α for point P in terms of E, A and B.

In this triangle,

$$\sin \epsilon = \sin E \sin B + \cos E \cos B \cos A. \qquad (1)$$

This gives ϵ to highest accuracy when ϵ is near zero, and lowest when ϵ is near $\pm 90^{\circ}$. However, for the latter case, the accuracy of a fix is usually very low anyway.

For small B, (1) approximates to

$$\sin \epsilon = \sin E \sin B + \cos E \cos A \quad . \qquad (2)$$

Also

$$\sin \alpha = \sin A \cos E / \cos \epsilon \quad . \qquad (3)$$

This gives α to high accuracy when α is near 0° or 180°, and low accuracy when α is near $\pm 90^{\circ}$.

Equation (3) can involve some ambiguity when there is a possibility of α lying outside the range 90° - 270°, which is very unlikely for normal pilot balloons. In this case, one can use the relation

$$\cos \alpha = (\sin \epsilon \sin B - \sin E)/(\cos \epsilon \cos B). \qquad (4)$$

This will give α more accurately around $\pm 90^{\circ}$, but less accurately around 180° or 0°. There will still be some ambiguity as to whether α lies in the range 0 - 180° or 180° - 360°, because $\cos \alpha = \cos (360^{\circ} - \alpha)$. However, this is easily resolved, because A and α will either both lie in the range 0 - 180° or both lie in the range 180° - 360°.

4. CALCULATION OF POSITION OF BALLOON

The polar coordinates of the balloon in the new system, (ϵ_1 , α_1) and (ϵ_2 , α_2), as seen from theodolites No. 1 and No. 2 respectively, are calculated. If $\alpha_1 = \alpha_2$, the readings are probably accurate and reliable. If $\alpha_1 \neq \alpha_2$, the balloon is most probably somewhere between planes No. 1 and No. 2, and also close to Ray No. 1 and Ray No. 2. If α_1 and α_2 do not differ much, the most likely location is on a plane for which α is somewhere between α_1 and α_2. At the required point in this plane, ϵ_1 and ϵ_2 will still have practically the same values as were calculated. This assumption (that ϵ_1 and ϵ_2 are virtually unchanged) is supported by the accuracy of results from this method, to be discussed later.

If $\alpha_1 \neq \alpha_2$, there must be some reason for this. Provided that the theodolites were set up properly, the most likely reason is limit of accuracy of the theodolites. In this case, if the theodolites are both read to the same accuracy, the angles determining the rays are liable to be in error by the same amount. For instance, if they are read to the nearest tenth of a degree, this error may be anything up to 0.05° for each instrument.

The effect of this error on the value of α can be deduced from the small spherical triangle in Fig. 4, in which two of the angles are close to 90°. If the position of the ray changes by angle δs, then $\delta\alpha$, the maximum error in α resulting from this, is given by $\sin \delta s / \sin \delta\alpha = \cos \epsilon / 1$, or $\delta\alpha = \delta s / \cos \epsilon$ for small δs and $\delta\alpha$. If the maximum permissible error (δs) is 0.05°, then the maximum error in α_1 is $\delta\alpha_1 = 0.05/\cos \epsilon_1$, while for α_2 it is $\delta\alpha_2 = 0.05/\cos \epsilon_2$, and so the maximum value of $|\alpha_1 - \alpha_2|$ is $\frac{0.05}{\cos \epsilon_1} + \frac{0.05}{\cos \epsilon_2}$.

Hence, if the discrepancy between α_1 and α is within limits of instrumental error, $|\alpha_1 - \alpha| \leq \frac{0.05}{\cos\epsilon_1} + \frac{0.05}{\cos\epsilon_2} = 0.05\left(\frac{\cos\epsilon_1 + \cos\epsilon_2}{\cos\epsilon_1 \cos\epsilon_2}\right)$,

or $0.05 \geq |\alpha_1 - \alpha| \frac{\cos\epsilon_1 \cos\epsilon_2}{\cos\epsilon_1 + \cos\epsilon_2}$. So, if the quantity $\psi = (\alpha_1 - \alpha_2) \frac{\cos\epsilon_1 \cos\epsilon_2}{\cos\epsilon_1 + \cos\epsilon_2}$ is calculated, and found to be smaller in magnitude than 0.05, the discrepancy can be attributed to limitations of instrumental accuracy, and the fix can be considered a good one.

If $|\alpha_1 - \alpha_2| \gg |\delta\alpha_1| + |\delta\alpha_2|$ (i.e. $|\psi| \gg 0.05$), it is possible that one of the theodolite scales has been misread, e.g. by 1° or 10°. Such an error can often be detected by inspection of the original data. Otherwise an optimum value of α is found by interpolating between α_1 and α_2 in the ratio $\delta\alpha_1$ to $\delta\alpha_2$.

This method of selecting the best value of α is, of course, quite arbitrary. If the discrepancy can be attributed to some other cause (e.g. balloon moving turbulently close to one theodolite, or passing overhead), a different method could be used.

Now that the new value of α is found, the position of the balloon in that plane can be found from ϵ_1, ϵ_2 and b, using the triangle shown in Fig. 5. If r_1 is the slant range of the balloon from theodolite No. 1,

$$r_1 = b \cos\epsilon_2 / \sin(\epsilon_1 - \epsilon_2). \qquad (5)$$

This triangle is indeed the best one to work with for finding the range of the balloon. In fact, the older graphical method (as described by Middleton and Spilhaus, 1958), in which the azimuth angles were plotted, merely involved working with the projection of this triangle on to the horizontal plane.

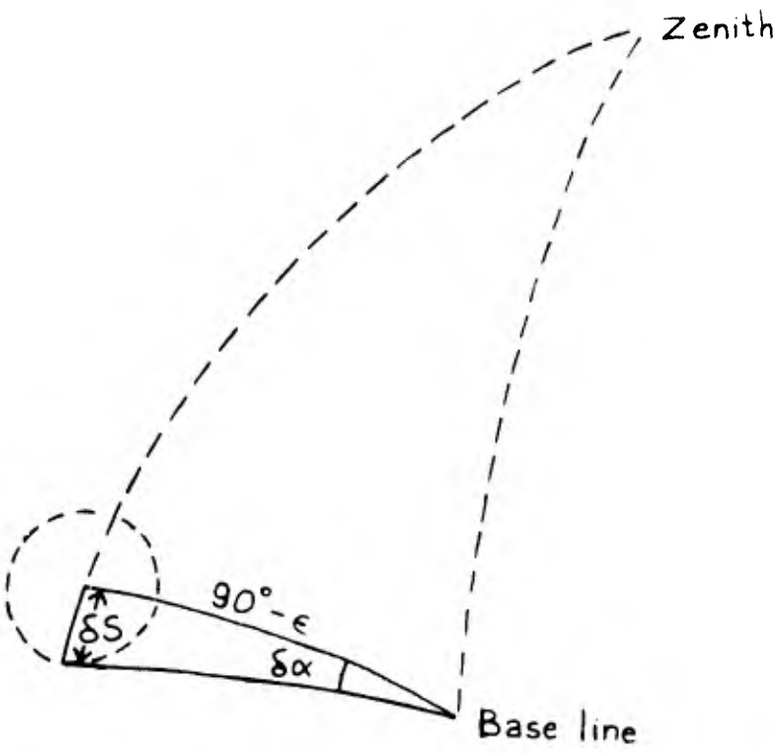

Fig. 4: Possible error in α ($\delta\alpha$) due to uncertainty δS in position of balloon.

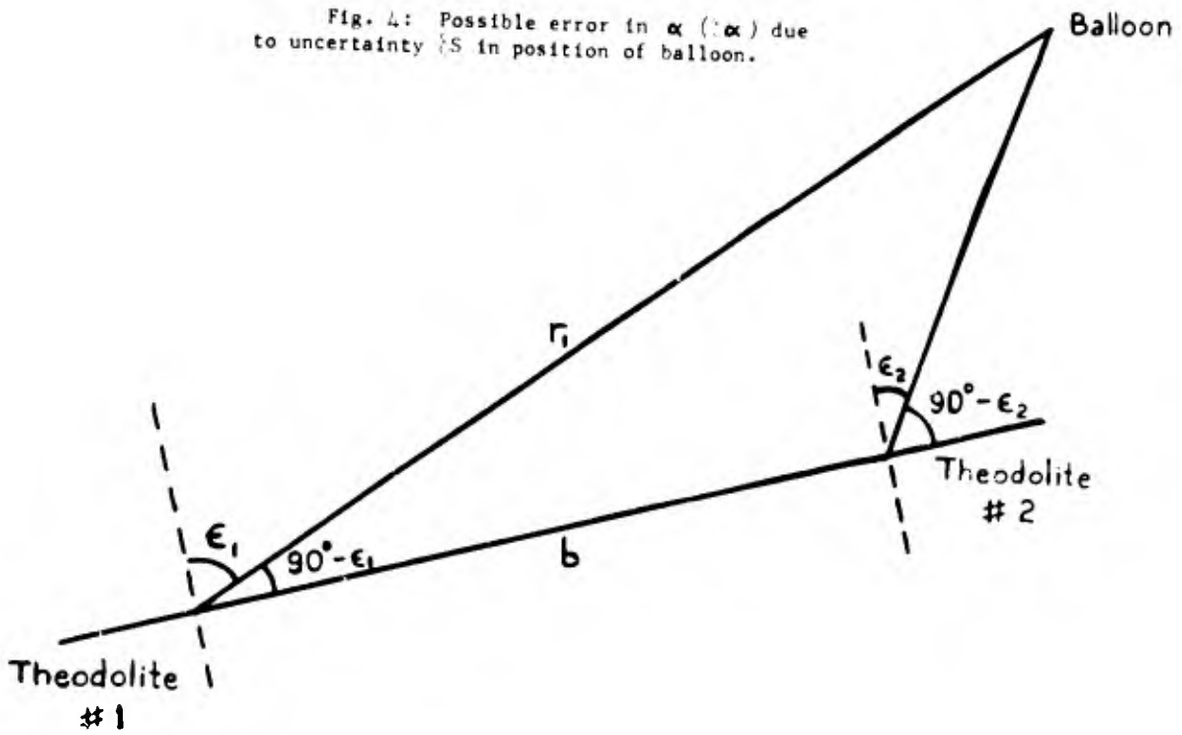

Fig. 5: Triangle for calculation of range of balloon.

The position of the balloon, in ordinary Cartesian coordinates relative to theodolite No. 1, can now be found from r_1, E_1 and A_1 (elevation and azimuth measured at theodolite No. 1) in the standard way. However, if α has been adjusted, the values of E_1 and A_1 are now slightly different from those originally measured, and corrections must be made. These can be found from appropriate relations linking E, A and α. From the triangle in Fig. 3,

$$\sin E = \sin \epsilon \sin B - \cos \epsilon \cos B \cos \alpha \qquad (6)$$

(no ambiguity, as $E \leqslant 90^\circ$ always)

and

$$\cos A = (\sin \epsilon - \sin B \sin E)/\cos B \cos E \qquad (7)$$

where A and α either both lie in the range $0 - 180^\circ$ or both lie in the range $180^\circ - 360^\circ$.

Alternatively, (6) and (7) can be differentiated, holding ϵ constant, to give the changes in E and A resulting from the adjustment to α. Approximating $\cos B \simeq 1$, they are

$$dE = \sin A \, d\alpha \qquad (8)$$

and

$$dA = \frac{dE}{\sin A} (\sin B - \tan E \cos A) = d\alpha (\sin B - \tan E \cos A) \; . \qquad (9)$$

5. CONSTRUCTION AND USE OF CHART FOR A GIVEN STATION

Computations by this method can be done by direct substitution of readings into the above equations. However, when many of them have to be done for a given base line, it may pay to compile a chart which will perform the transformation from the (E,A) coordinate system into the (ϵ , α) system and vice-versa.

To make the chart, values of ϵ and α are calculated which correspond to standard values of E and A (e.g. at 1° intervals, with larger intervals near the zenith). Equations (1) to (4) can be used. Alternatively, one can select standard values of ϵ and α , and use equations (6) and (7) to find the corresponding values of E and A.

The axes used for plotting the chart are arbitrary. For example, E and A can be plotted as polar coordinates, with lines of constant A radiating from the origin and lines of constant E as concentric circles with regular spacing, $E = 90^\circ$ coinciding with the origin. The lines of constant ϵ and α will now form a pattern identical to the lines of latitude and longitude on a great circle map centred on a place at latitude B. Some types of upper wind plotting board could be adapted to make this type of chart (e.g. Department of Transport Plotting Board Type 3). This mapping involves less distortion than the others which follow.

Alternatively, ϵ and α can be plotted on Cartesian axes. This projection is more difficult to construct and use where ϵ approaches 90°. Cases of α outside the range 90° - 270° will be rare, unless the base line slopes considerably. This type of plot is symmetrical about the point E = 0, $A = 90^\circ$.

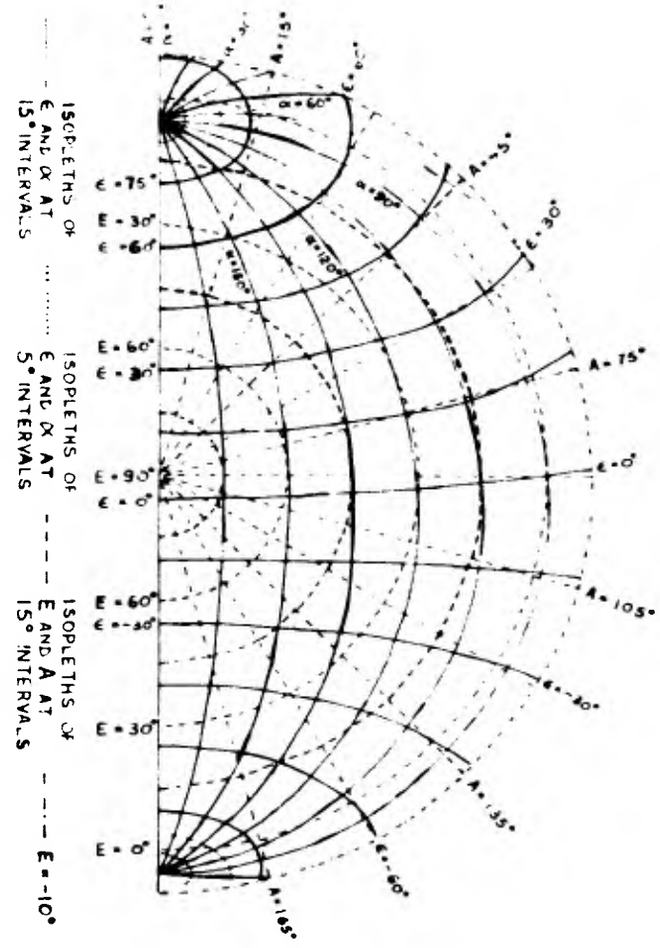

Fig. 6a: Isopleths of ϵ and α, in terms of E and A, with E and A in polar coordinates. Slope of base line = 6°.

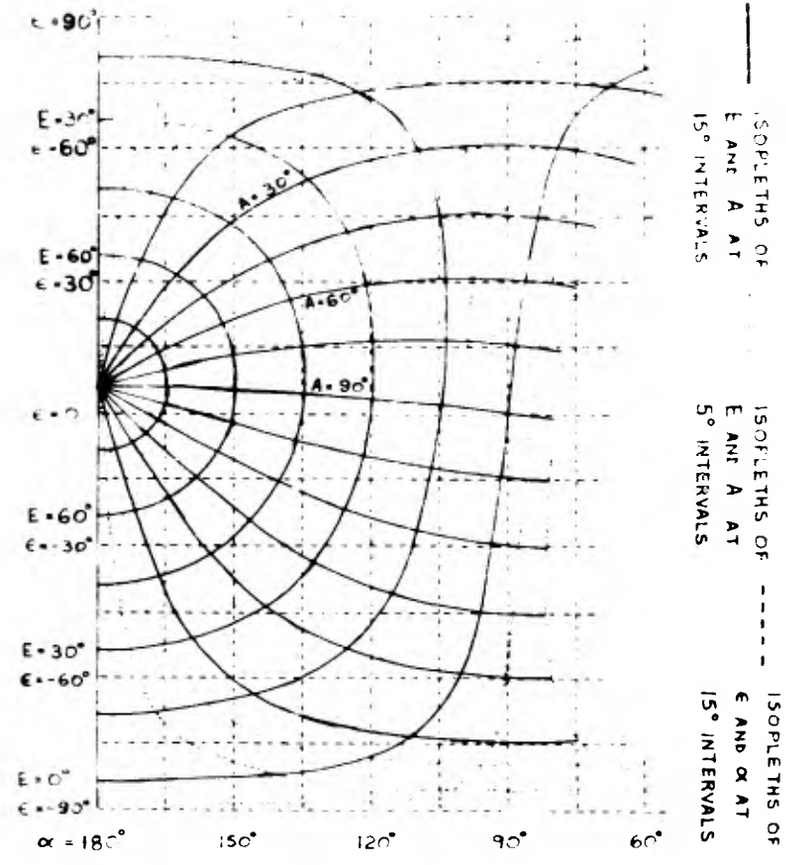

Fig. 6b: Isopleths of E and A, in terms of ϵ and α, with ϵ and α in cartesian coordinates. Slope of base line = 1°.

Simplified examples of these charts are shown in Fig. 6. As the diagrams are symmetrical about the line A = 0 or $\alpha = 180^{\circ}$, it is only necessary to plot the graph for one side of this line.

In use, the point corresponding to the given values of E and A is found on the chart, and the corresponding values of ϵ and α are read off.

6. UNIVERSAL CHARTS FOR USE AT ANY STATION

The above method gives a chart which can be used for only one angle of slope of the base line. If only a few calculations are to be made for a given base line, preparation of a special chart is hardly worthwhile. For this case, a chart designed for use with any base line may be preferred. Such a chart has the further advantage that the computation involved in compiling it is simpler, and the disadvantage that a single graph will not cover the full field of view satisfactorily.

To understand the principle of the universal chart, it is helpful to refer to Fig. 2, and imagine the two coordinate systems inscribed on two close-fitting, concentric spheres. If the outer sphere is transparent, then it is possible to read off the corresponding values of (E,A) and (ϵ , α) for any point. By rotating one globe relative to the other about a line OH which is perpendicular to the axes OL and OZ of the two globes, the value of B can be changed as desired. (If B is made equal to 90°, then points L and Z will coincide, and indeed the (E,A) and (ϵ , α) coordinate systems will coincide completely.)

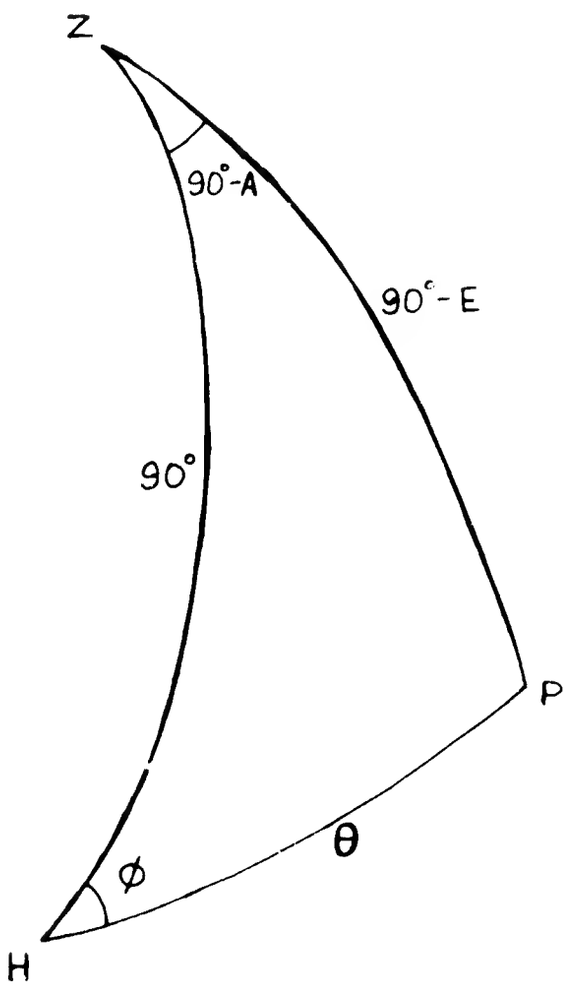

Fig. 7: Spherical triangle ZPH.

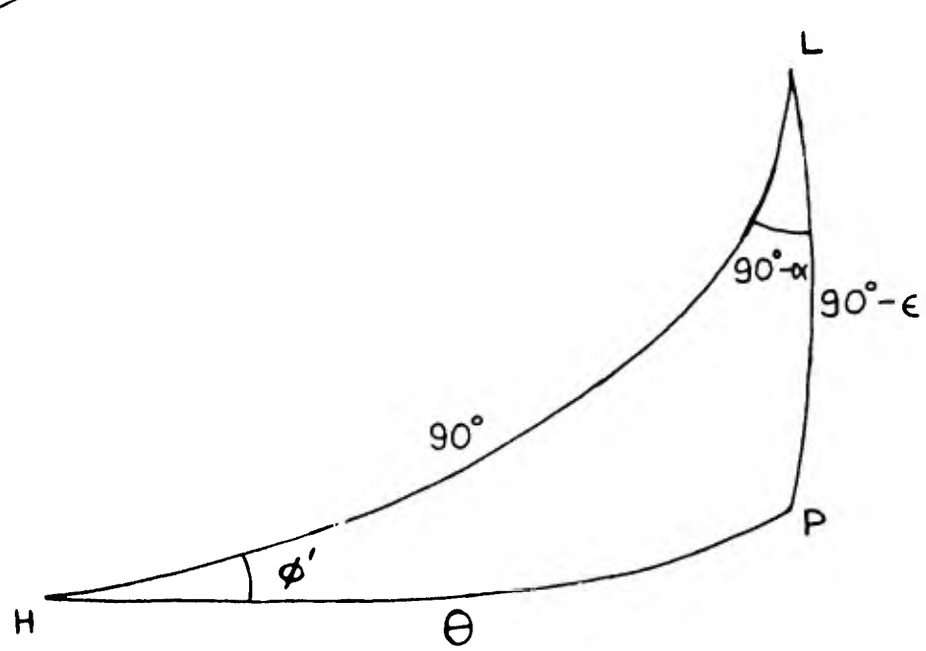

Fig. 8: Spherical triangle LPH.

Two real globes, big enough to give the desired accuracy, would be inconvenient to make and store. Therefore, just as the cartographer projects the earth's surface on to other surfaces in making his maps, we shall try to project each sphere on to suitable plane or cylindrical surfaces, such that a rotation about axis OH will produce a proportionate shift in the projection. This is possible by projection on to a cylinder whose axis corresponds to OH and which is therefore tangential to the sphere along the great circle ZLN. Mercator's projection would be suitable (using ZLN as the "equator"), or, indeed, any other in which the merid ans are linearly spaced. This projection will not cover the region near H. For this region, a polar-type projection on to a plane tangential to the sphere at point H is preferable. It could be gnomonic or equidistant azimuthal, for example.

For construction of the "latitude and longitude" lines of the (E,A) system on the planes of projection, consider the spherical triangle ZPH shown in Fig. 7, where P is any point (E,A) in this system. If side PH is of length θ, and angle ZHP is called ϕ, then, as $ZH = 90^\circ$,

$$\cos \theta = \cos E \sin A$$

and

$$\cos \phi = \sin E / \sin \theta \quad .$$

Point P is at angular distance $(90^\circ - \theta)$ from the great circle ZL. Therefore, in the cylindrical projection, its distance x from line ZL on the chart can be made proportional to $(90^\circ - \theta)$, or any function of $(90^\circ - \theta)$. (E.g. $x \propto \cot \theta$ if O is used as the point of projection.) The scale of ϕ should be linear and in the ZL direction. This projection should be used for values of θ from 90° down to 45° or less.

The chart for points close to H can be plotted on a polar basis. The distance r of P from the origin can be made proportional to θ (as in the

equidistant azimuthal projection) or to any function of θ (e.g. $r \propto \tan \theta$ for a gnomonic projection). ϕ is the polar angle.

In the same way, the "latitude and longitude" lines of the (ϵ , α) system can be drawn on the planes of projection. From spherical triangle LPH (Fig. 8), where PH is still of length θ, and angle LHP is called ϕ' ,

$$\cos \theta = \cos \epsilon \sin \alpha$$

and $$\cos \phi' = \sin \epsilon / \sin \theta \ .$$

These are identical in form to the equations which give θ and ϕ from E and A. Therefore the pattern of "latitude and longitude" lines of ϵ and α , as related to the point L, is identical to the pattern for E and A as related to the point Z.

So this one pattern can be drawn on two different sets of sheets, representing the (E,A) and (ϵ , α) families of lines. One set of sheets should be transparent, and laid over the other so that L is at (90°-B, 0) in the (E,A) system and Z is at (90°-B, 180°) in the (ϵ , α) system. On both the cylindrical and polar projections, lines of constant ϕ and ϕ' should coincide, and at any point, $\phi - \phi' = 90^\circ$-B. Anywhere on the graph, corresponding pairs of coordinates in the two systems can be read off.

The relationship just given between ϕ and ϕ' can be used as the basis of a still simpler method, which requires only one graph to be plotted for each of the two projections. Transformation from the (E,A) to the (ϵ , α) system can be divided into 3 steps:

(1) Transform from (E,A) to (θ,ϕ)

(2) Subtract (90°-B) from ϕ to give ϕ', and leave θ unchanged

(3) Transform from (θ,ϕ) to (ϵ , α) using the same graph.

From another point of view, from Fig. 9 we can see that the position of P relative to the (ϵ , α) coordinates based on L is the same as that of point Q relative to the (E,A) coordinates based on Z, where the value of ϕ at Q is (90^{o}-B) less than its value at P.

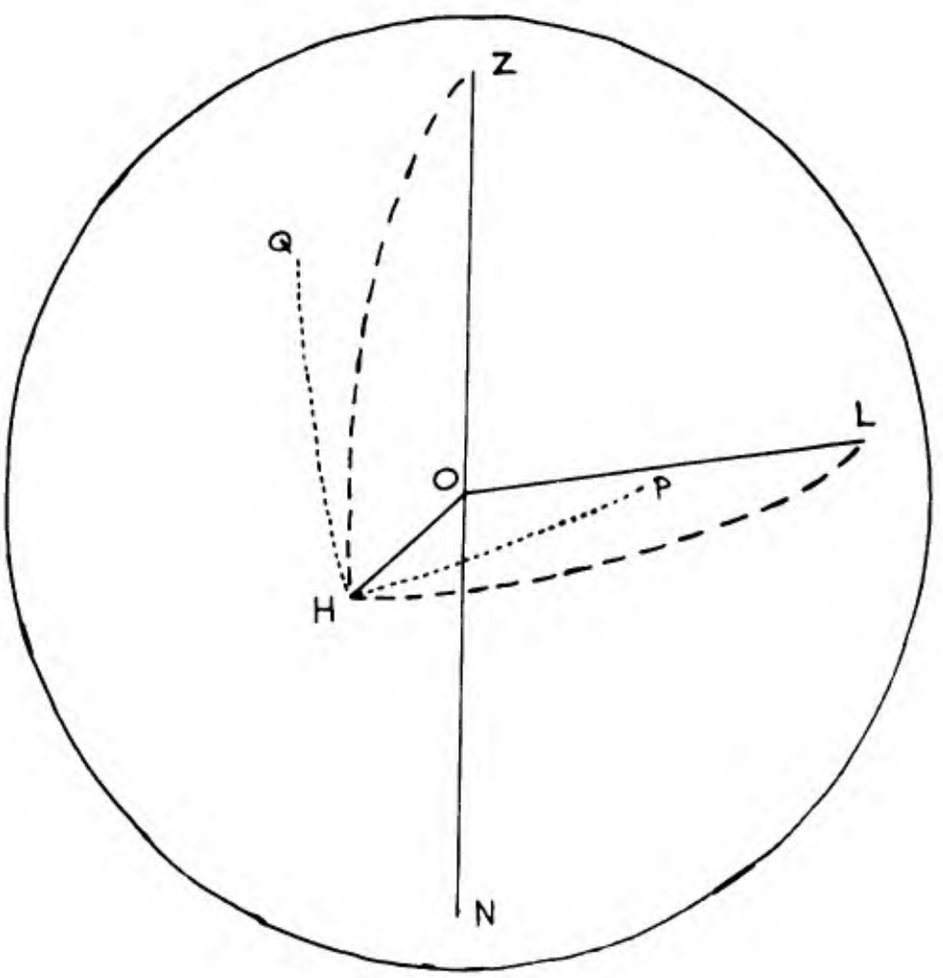

Fig. 9: Point P is in the same position relative to LH as point Q is relative to ZH, where angle PHQ = 90^{o} - B.

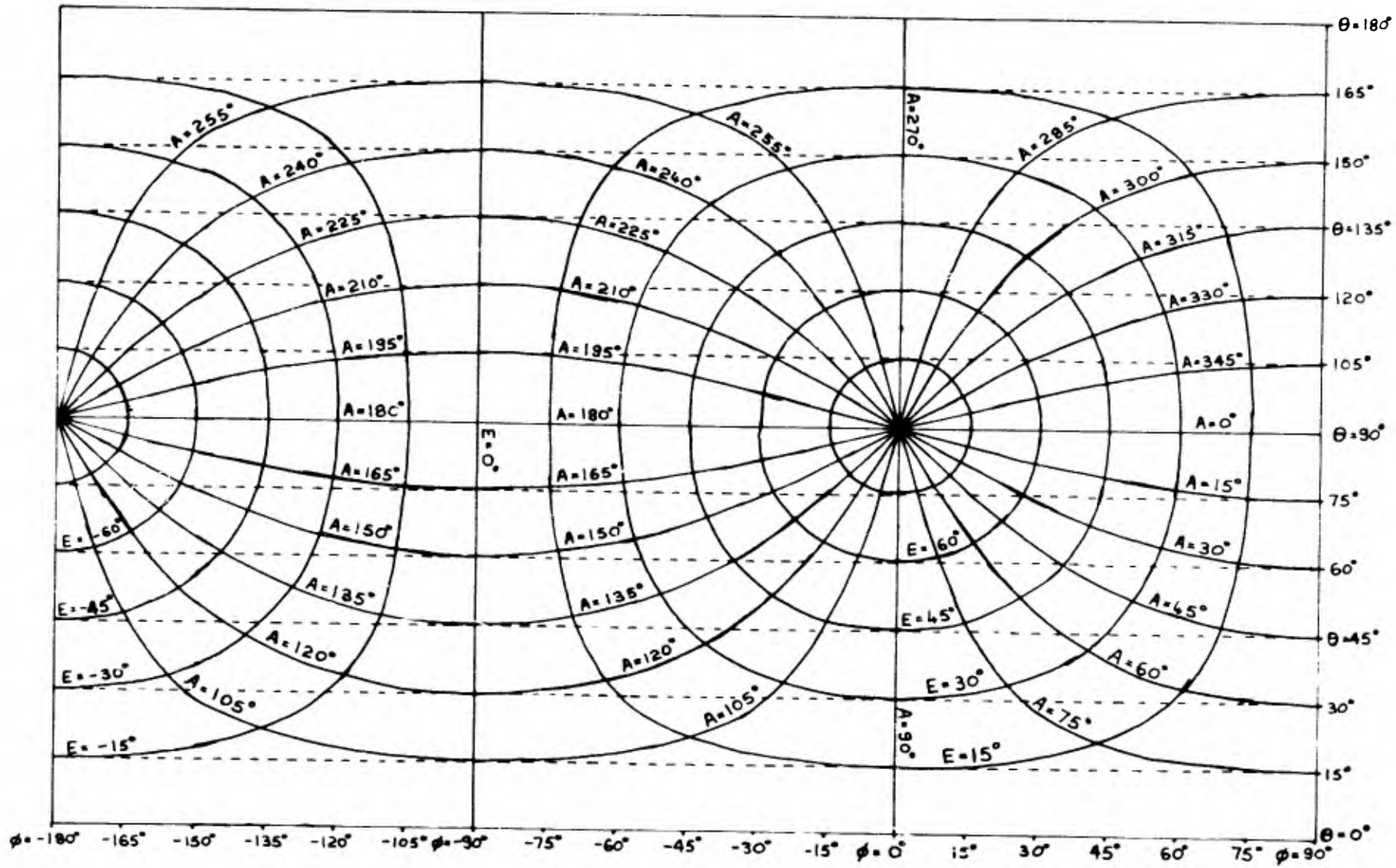
A=255°
A=240°
A=225°
A=210°
A=195°
A=180°
A=165°
A=150°
A=135°
A=120°
A=105°
E=-60°
E=-45°
E=-30°
E=-15°
E=0°
A=270°
A=285°
A=300°
A=315°
A=330°
A=345°
A=0°
A=15°
A=30°
A=45°
A=60°
A=75°
A=90°
E=60°
E=45°
E=30°
E=15°
θ=180°
165°
150°
θ=135°
120°
105°
θ=90°
75°
60°
θ=45°
30°
15°
θ=0°
φ=-180°
-165°
-150°
-135°
-120°
-105°
φ=-90°
-75°
-60°
-45°
-30°
-15°
φ=0°
15°
30°
45°
60°
75°
φ=90°

On the cylindrical projection, subtraction of ϕ can be done by using a ruler with two marks on it corresponding to a change in ϕ of $(90^{\circ}-B)$. (See Fig. 10) The ruler is laid parallel to lines of constant θ. On the polar projection, some sort of protractor could be used to subtract ϕ. The graph should cover a range of ϕ from 90° to -180°, or even more if negative elevation angles are likely to occur. Because of symmetry, it is only necessary to calculate θ and ϕ for values of E and A between 0° and 90°.

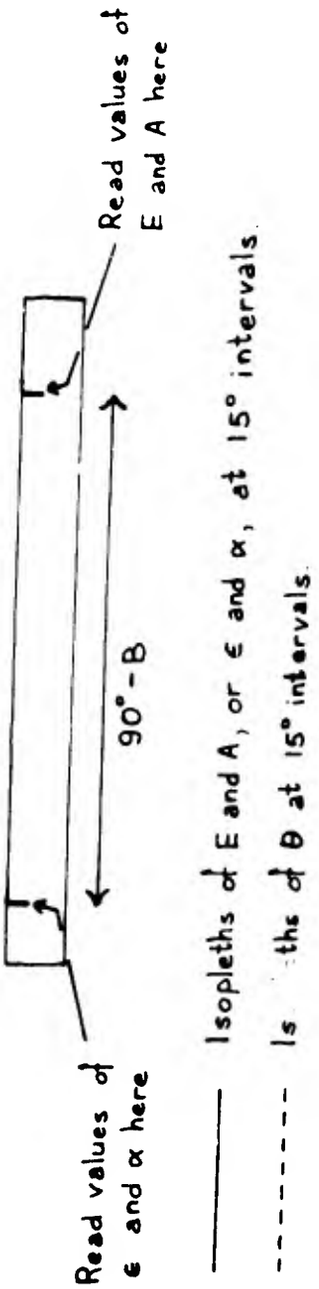

Fig 10: A simplified "universal chart" opposite, with ruler shown on this page.

7. GENERAL PROCEDURE FOR USE OF CHARTS

Using one of the charts described in Sections 6 and 7, ϵ and α are found for both of theodolites No. 1 and No. 2. The values ϵ_1 and ϵ_2 are used to find the slant range r_1, either from Eq. (5) or graphically. The values α_1 and α_2 are used to estimate a "corrected" value of α, as suggested in Section 4 or otherwise. From ϵ_1 and the corrected value of α, the "corrected" values of E_1 and A_1 are found from the chart, and used to find the balloon's position. Henceforth, any standard method can be used to calculate the wind speed.

8. CONCLUSION

This method eliminates the arbitrary choice of three of the four coordinates which is involved in the old graphical method of double theodolite pibal computation, as described, e.g., by Middleton and Spilhaus (1953). It is not superior in accuracy to the author's computer method described in 1962. However, the approximations involved (e.g. assumption that ϵ_1 and ϵ_2 need not be changed in estimating the balloon's most likely position) will only cause a significant loss of accuracy in cases where the data are unreliable anyway (e.g. if α_1 and α_2 differ greatly).

For a comparison of accuracy and speed, a given run of 40 readings, made on a base line 1593m long, was calculated completely on an IBM 7044 computer by both the new method and the previous one (Thyer, 1962). By the

new method, it took 0.06 minutes to execute, whereas by the older method it took 0.09 minutes. (However, the author has reason to distrust the execution times printed by this particular computer.)

The outputs printed the height and horizontal distance of the balloon for each reading. Amongst those readings which were consistent within the limits of instrumental error, the greatest discrepancy between the two methods was 2 metres at a horizontal range of 13200m, and 1m in a vertical height of 2800m. In the worst reading of the run, where the angular errors totalled over 4^{o} (40 times the permissible error) and the rays from the two theodolites were 107m apart at their closest, the corrected horizontal ranges given by the two methods differed by 4m at a distance of 1280m, and the heights by 4m at an altitude of 790m.

The greatest advantage of the new method is its applicability to chart calculation, which is useful when quick results are wanted in the field and a computer is not handy. The original compilation of the chart is a tedious job requiring high accuracy, in which as many automatic aids as possible may be desired. However, once compiled, the chart can be used for any number of ascents, and with the aid of standard slide rule or plotting board, fairly rapid calculations of wind speed should be possible.

REFERENCES

Middleton, W.E.K., and A.F. Spilhaus, 1953: Meteorological Instruments, University of Toronto Press, 286 pp. (Ch. 7, 186-187).

Thyer, N.H., 1962: Double theodolite pibal evaluation by computer. J. Meteor., 1, 66-68.

APPENDIX

Worked Example:

For the run made at Penhold, Alberta, at 1115MST, 27 July 1966.

Horizontal length of baseline = 1593m.

Theodolite No. 2 is 6m lower than No. 1

$\therefore$ Angle of slope of baseline $B = \tan^{-1} \frac{-6}{1593} = \tan^{-1} -0.00376 = -0.22^{\circ}$.

Length of baseline $b = ((1593)^2+(6)^2)^{1/2} = 1593$

At time 6.5 min after release of balloon,

$A_1 = 107.4^{\circ}$ $E_1 = 61.8^{\circ}$ $A_2 = 161.1^{\circ}$ $E_2 = 32.6^{\circ}$

As $|B|$ is small, we can use equation (2) to find ϵ .

This gives $\sin \epsilon_1 = \sin E_1 \sin B + \cos E_1 \cos A_1$

$= \sin 61.8^{\circ} \sin (-0.22^{\circ}) + \cos 61.8^{\circ} \cos 107.4^{\circ} = -.14466$

$\therefore \epsilon_1 = -8.32^{\circ}$

and $\sin \epsilon_2 = \sin E_2 \sin B + \cos E_2 \cos A_2$

$= \sin 32.6^{\circ} \sin(-0.22^{\circ}) + \cos 32.6^{\circ} \cos 161.1^{\circ} = -.79909$

$\therefore \epsilon_2 = -53.04^{\circ}$

We now use equation (3) to find

$\sin \alpha_1 = \sin A_1 \cos E_1 / \cos \epsilon_1 = \sin 107.4^{\circ} \cos 61.8^{\circ} / \cos (-8.32^{\circ})$

$= .45572$

$\therefore \alpha_1 = 152.89^{\circ}$

and $\sin \alpha_2 = \sin A_2 \cos E_2 / \cos \epsilon_2 = \sin 161.1^{\circ} \cos 32.6^{\circ} / \cos (-53.04^{\circ})$

$= .45387$

$\therefore \alpha_2 = 153.01^{\circ}$

These values could also have been found directly from a chart, as described in section (5) or (6).

Our two values of α do not agree exactly. $\alpha_1 - \alpha_2 = -0.12^\circ$ and

$$\psi = -0.12 \left(\frac{\cos(-8.32^\circ)\cos(-53.04^\circ)}{\cos(-8.32^\circ) + \cos(-53.04^\circ)}\right) = -0.045$$

As $|\psi| < 0.05$, this means that our discrepancy $\alpha_1 - \alpha_2$ can be attributed to limits of instrumental accuracy when the original readings are made only to the nearest tenth of a degree and are therefore liable to an error of 0.05°. Therefore the original readings were satisfactory, and there is no need to adjust them. We can therefore use the original values of E_1 and A_1 to compute the position of the balloon.

From Eq. (5), the slant range from theodolite No. 1 is

$$1593 \cos(-53.04^\circ)/\sin(-8.32^\circ - (-53.04^\circ)) = 1361\text{m} .$$

Therefore vertical height above theodolite No. 1 is $1361 \sin E_1\text{m} = 1199\text{m}$. Horizontal distance from theodolite No. 1 is $1361 \cos E_1\text{m} = 643\text{m}$ and azimuth $= A_1 = 107.4^\circ$.

For time 5.5 min after release, slightly different treatment of the readings is advisable, because $|\psi|$ turns out to be larger. Here, $A_1 = 125.0^\circ$, $E_1 = 63.0^\circ$, $A_2 = 169.0^\circ$, $E_2 = 28.5^\circ$.

By the same method, we find $\epsilon_1 = -13.15^\circ$, $\epsilon_2 = -59.81^\circ$.

$$\alpha_1 = 160.80^\circ \qquad \alpha_2 = 160.52^\circ$$

So $\alpha_1 - \alpha_2 = 0.28^\circ$ and $\psi = 0.093$.

Now $|\psi| > 0.05$, so the agreement between readings is not so good. In this case, for the best estimate of α we interpolate between the calculated values of α_1 and α_2 in the ratio $\xi\alpha_1$ to $\xi\alpha_2$.

$\xi\alpha_1 = \dfrac{0.05}{\cos\epsilon_1} = 0.05$ $\quad$ $\xi\alpha_2 = \dfrac{0.05}{\cos\epsilon_2} = 0.10$, so the interpolated value of α is $\dfrac{0.05}{0.05 + 0.10} = 1/3$ of the way between α_1 and α_2, viz. $\underline{160.71^\circ}$.

Using this new value of α and the original value of ϵ_1, we can now find new values for E_1 and A_1, either from a chart or from equations (6) and (7).

Using these equations,

$$\sin E_1 = \sin(-13.15^\circ)\sin(-0.22^\circ) - \cos(-13.15^\circ)\cos(-0.22^\circ)\cos 160.71^\circ$$

$$\therefore \quad E_1 = 66.9^\circ$$

$$\cos A_1 = (\sin \epsilon_1 - \sin B \sin E_1)/\cos B \cos E_1$$

$$= (\sin(-13.15^\circ) - \sin(-0.22^\circ)\sin 66.9^\circ)/\cos(-0.22^\circ)\cos 66.9^\circ$$

$$= -.5711$$

$$\therefore \quad A_1 = 124.8^\circ$$

Just as in the previous example, the slant range is computed from ϵ_1 and ϵ_2, and the vertical height and horizontal distance from the <u>new</u> values of E_1 and A_1.

CONTINUITY IN HAIL PRODUCTION AND SWATHS

A REVIEW

by

Jerry Pell

CONTENTS

BLANK PAGE

CONTINUITY IN HAIL PRODUCTION AND SWATHS

A REVIEW

Jerry Pell

ABSTRACT

The Wokingham storm study made by Browning and Ludlam postulated a steady-state "supercell" which would generate hail continuously along the storm trajectory. Although such storms may very well exist, or as Browning and Fujita point out, some storms may attain a quasi-steady state for certain portions of their lifetimes, there are documented cases of storms which produce intermittent hailswaths, disrupted by patches of only rain. In particular, we may mention the work of Carte in both Africa and Alberta, and of McBride in Alberta.

Closely related to the problem of swath continuity is that of continuity of hailfall at a point. Again, reliable reports have been received from observers who indicate that frequently hail may fall in "bursts", separated by periods of either rain or no precipitation at all.

1. INTRODUCTION

One of the more frequently abused words in the literature on severe storms has been the term "continuity". Too seldom is the context in which it is used explicitly stated. With respect to hail and its production, there is a clear distinction to be made between the concept of continuity as the hailfall appears on the ground, and that of continuity as applied to hail production aloft.

Let us first consider the ways in which we might investigate the presence or absence of continuity in the generating cell itself, as observed on radar and by inference from ground observations. The very word "cell" has suffered a sufficiently varied usage to justify definition; for the purpose

of this article the term shall be used to denote a single set of closed concentric contours of effective radar reflectivity (Z_e), increasing monotonically in value toward a central region or core. The simplest criterion of cell continuity is merely its continued existence as a radar echo for a specified period of time. We may now add as a requirement for continuity the constancy of the core value of Z_e. The next step is to look at the production of hail by this cell and establish the cell's nature as a generator, a task for which the present state of the radar art is insufficient and surface observations are required.

Assuming the presence of a high-density observing network (say, one report per square mile), a necessary requirement for continuous hail would be the verification of hailfall at all stations along the swath, with no gaps. The study may then be refined to include data on the constancy among all the stations of both the hail size distribution and intensity. Also included is the problem of point-hailfall continuity, which is the requirement of a single uninterrupted hailfall at each individual observation point.

If a single cell were to fulfill all of the afore-mentioned criteria (admittedly severe), it could then be called a "steady-state generator" in the fullest sense. However, the typical hail-producing frontal thunderstorm system is a complex organization of interacting cores, and requires careful study to be adequately understood. For example, several non-continuously generating cells might combine in sequence to produce a continuous swath of hail at the ground. Each cell could itself be quite short-lived, but a ground observer without radar would be unable to distinguish the hailfall so produced from that of a single continuous steady-state generator. Problems such as this are explored further in the following sections.

The phrase "hail cell", as used in this paper, refers to a set of surface observations of hailfall which may be identified as distinct from other patches of hail in the same swath, the hail cells being separated by areas of no hailfall, usually verified to some degree by ground reports.

2. HAILSWATH CONTINUITY

2(i) Douglas and Hitschfeld; Browning and Ludlam

The concept of a steady-state hail-generating mechanism which lays down a continuous swath of hail has found much favour in the literature. Douglas and Hitschfeld (1958, 1959) presented radar data of persistent echo-top heights (about 30 kft) in Alberta storms as an argument for continuity. Elsewhere, a steady-state storm model which has attracted much attention, based on a study of the Wokingham, England, storm (Browning and Ludlam, 1960, 1962; Ludlam, 1963) describes a process whereby hail is being continuously generated. A picture of this model, after Browning (1965), is reproduced here as Figure 1. Further evidence to support this model was provided by Hitschfeld and Douglas (1961) in the form of hail reports received from volunteer observers, which seemed to indicate that, in about 75% of the 43 major storms which occurred over a three year period, "the hail fell for protracted periods and was spread out over narrow elongated strips". However, an examination of their data reveals that, for a median strip length and width of 50 and 10 miles, respectively, the information

density is only about 0.1 reports per square mile. Douglas (1961), writing elsewhere in the same publication, called attention to this limitation, noting that although "storms have been observed in Alberta in which a single cell alone has apparently produced more or less continuous hail...the continuity is open to question, since it is not clear whether gaps in the swath are indicative of faults in the reporting network or of true lulls in hail production." The difficulty lies in a lack of reports of "no hail" (Douglas, 1963), which, if available, would confirm and delineate any true breaks in the hail swath.

2(ii) Changnon and Stout

Changnon and Stout (1962) found that hail cell patterns and dimensions at the surface in Illinois were highly variable, pointing out that "many presently defined hailstorms and hailswaths may actually be a composite of many hail cells which, because of their close proximity in time and space, result in their eventual depiction as single continuous swaths of hail". This conclusion was arrived at from a study of six hail cells, varying in size up to a maximum of 6.6 square miles, based on a high observer-density of about one report per square mile. The six cells studied were defined by maps of the instantaneous hailfall at five-minute intervals during the storm. A study of these and other hail cells revealed many to be elliptical with typical axial lengths of 4 and 2 miles for the major and minor axes, respectively. Since the authors did not map out the actual reports, it is impossible to study their hail cell contours in detail, but since they used an extremely short time interval, Changnon and Stout clearly placed great faith in the observers' reported times of hail onset and duration. This degree of confidence has not been shared by other researchers, who have found strong biases (for example, toward quarter-hour multiples) in

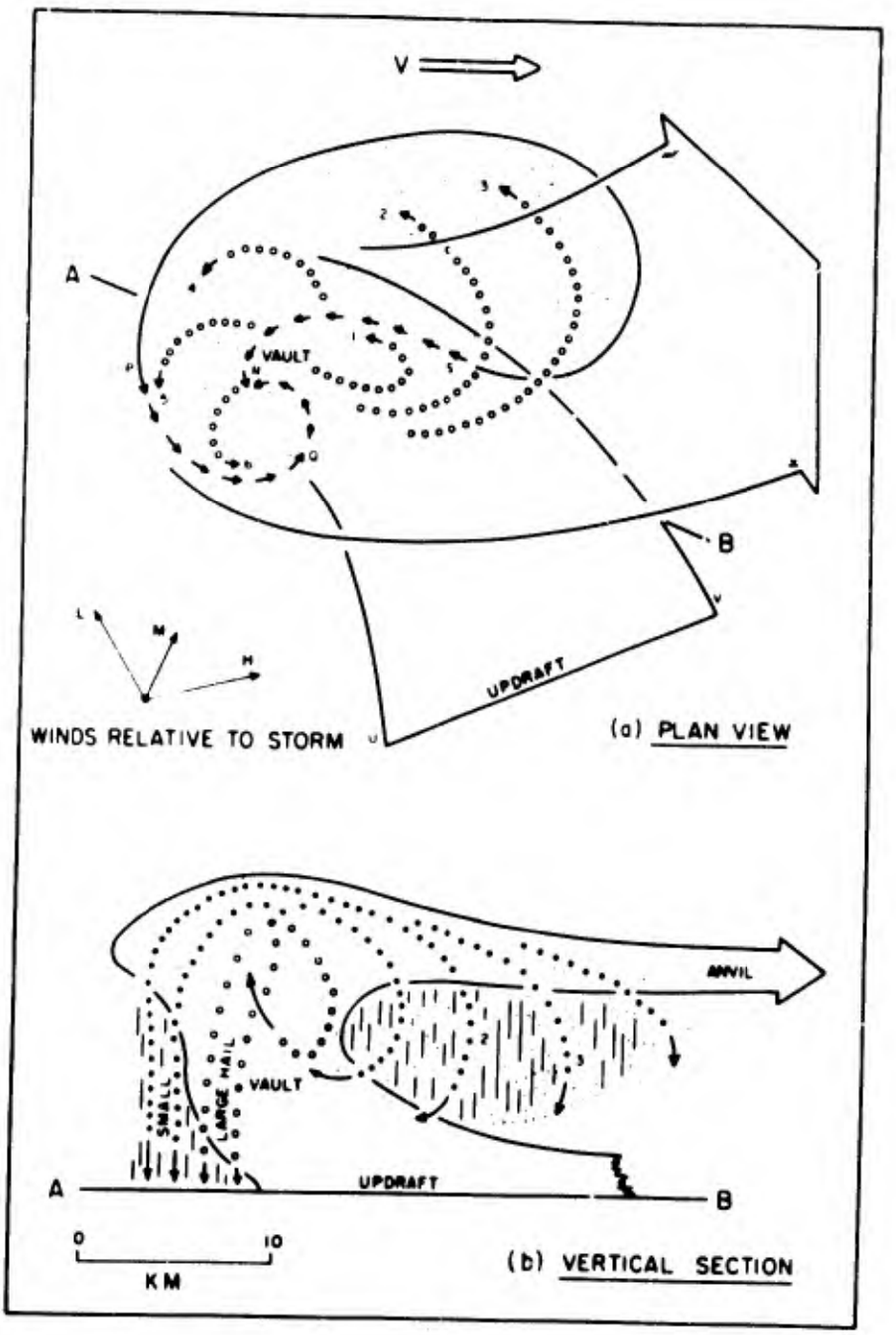

Fig. 1: Schematic horizontal (a) and vertical (b) sections qualitatively illustrating precipitation trajectories in different parts of an SR storm (S for Severe, and R for travelling to the Right) travelling at a velocity V. In both figures the extent of the updraft is represented by solid curves; precipitation trajectories are represented by dotted curves. In (a), the extent of rain and hail close to the surface is represented by light and heavy shading respectively, and the arrows around PQRS indicate the direction of protuberances on the edge of the low-level radar echo. AB is oriented in the direction of the mean wind shear, into which the updraft is inclined at low and medium levels. In (b), the presence of downdrafts with strong normal components of motion is indicated by broken vertical hatching. On the downshear side of the updraft (right side of page) these components are directed into the page; beneath the updraft on its upshear side they are directed out of the page. From Browning (Browning and Fujita, 1965).

reported times (Donaldson et al, 1960; Douglas, 1961; Carte, 1963; Williams and Douglas, 1963; McBride, 1964; Carte, 1966; and others).

2(iii) Schleusener and Henderson

Schleusener and Henderson (1962) found that separate hailfalls within a storm are of short average duration (4.6 minutes), which suggested to them the presence of "small-scale hail shafts within various portions of the precipitation cell".

2(iv) Carte

The first study specifically intended to determine the continuity characteristics of hailswaths was undertaken by Carte (1963), who used data collected by the Alberta Hail Studies Project. He concentrated on 12 storms of at least moderate severity, whose characteristics may be summed up as follows:

TABLE 1

Summary of twelve Alberta hailstorms studied by Carte (1963)

	RANGE	AVERAGE
Swath Length:	55 - 120 mi.	88 mi.
Swath Width:	4 - 20 mi.	10 mi.
Number of Hail Reports:	90 - 226	158
Total Hailstorm Duration:	145 - 355 min.	203 min.
Point-Hailfall Duration:	9 - 18 min.	13 min.
Velocity of "Hail Cell"*:	23 - 42 mph.	28 mph.

*Note: A "hail cell" in this context is defined by Carte as the area on which hail was falling at a given instant.

Therefore, on the basis of the "average swath", Carte had an average hail-report data density of about 0.2 reports per square mile, which is quite low in comparison to the more desirable density of one report per square mile.

Comparing his results with those of Changnon and Stout (1962), Carte found that "the principal differences between the Illinois and Alberta hail cells appear to be that in Alberta cell sizes are much larger (4 - 20 miles across), and the bigger hail tends to be closer to the leading edge. Alberta hail cells, as those in Illinois, were on the right (south) of the main area of precipitation, as indicated by the radar".

Carte reiterated the problem of the lack of reports of no hail to verify true breaks in the swath, and went on to show that the assumption of continuity on the basis of sparse observer reports and persistent steady radar echo is often unjustified. Working on the premise that a farmer who has volunteered data in the past would reliably report subsequent occurrences of hail, he developed, for any specific storm, the expression

$$P = \frac{c}{b} = \frac{a}{x} \quad ,$$

where x is the total number of active hail reporters randomly distributed over area A,
b is the number of observers who have reported hail previously (included in x),
a is the number of reports received from the specific storm, and
c is the number of reports (included in a) which came from the b observers,

so that P is the probability of hail from this storm falling at any given point within the area A. Since a, b, and c are known, both P and x can be readily calculated. Thus, even though all x observers have not reported (i.e. have not experienced hail), we can determine x for different regions. Carte found a range of values from 1.2 to 0.1 or less per square mile, with

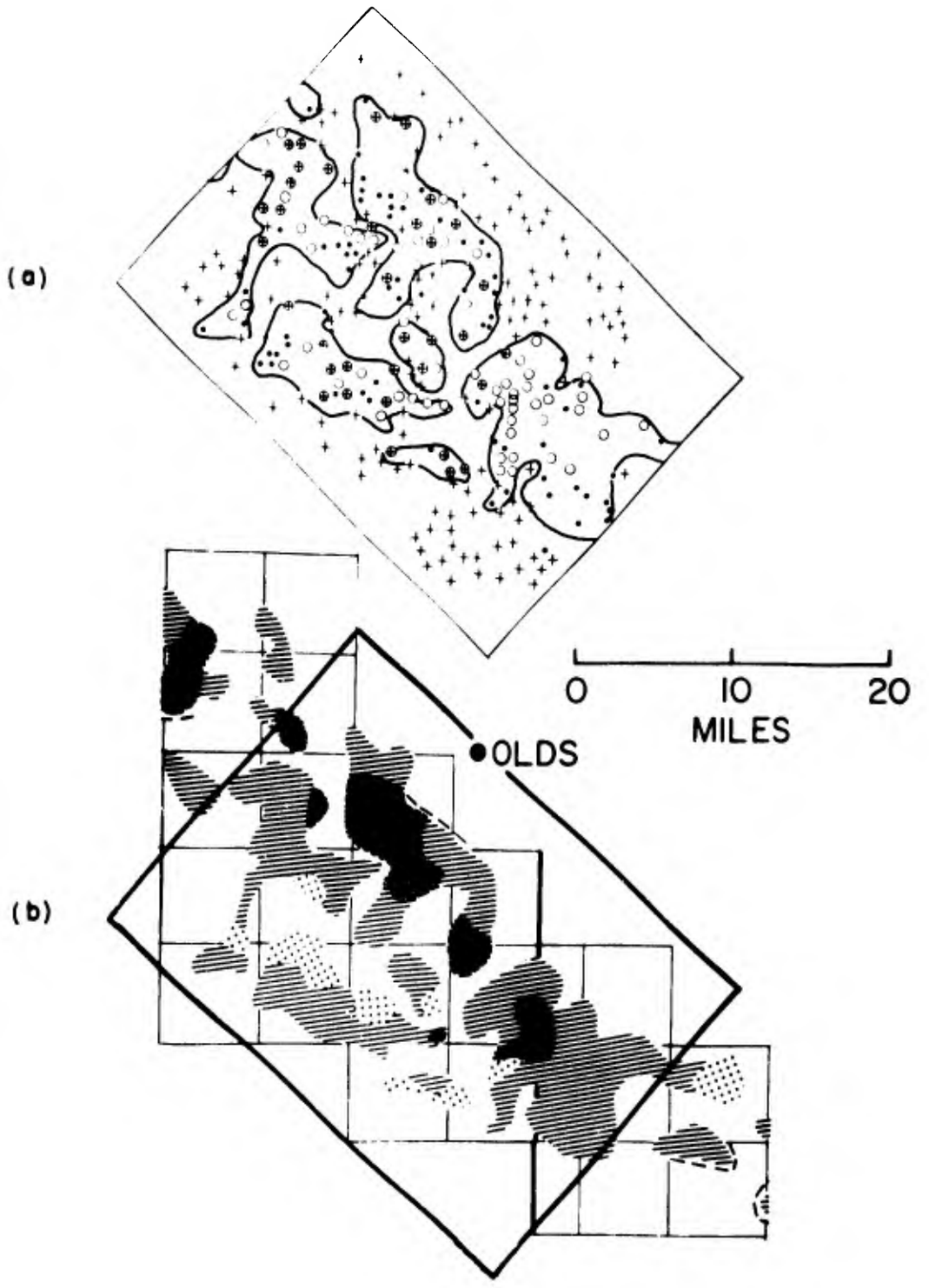

Fig. 2: Carte's analysis of part of the 26 August 1959 Alberta hailswath.
(a) Outline of part of the swath, and the raw data on which this outline is based: ⊙ signifies card reports of hail on August 26, 1959, + indicates card reports on days in 1959 other than August 26, ⊕ signifies card reports of hail on August 26 and at least one other day, and ● shows insurance reports of hail on August 26.
(b) Part of the swath in its final stage of analysis, with shading suggesting maximum hail size as follows: ⁘ indicates Small hail (less than 1 cm diameter), ▤ represents Medium hail (1 to 3 cm diameter), and ■ shows Large hail (greater than 3 cm diameter). Oblique rectangles in (a) and (b) cover the same area.
From Carte (1963).

an average for the entire project area of 0.3 active hail reporters per square mile. He went on to conclude that judging continuity on the basis of hail-report density was therefore misleading because of the large variability in the number of observers from region to region. The above technique may be criticized on the grounds that the assumptions of (1) the randomness in the distribution of active hail reporters, and (2) the continuing reliability of all of these volunteers, are both open to question. Much of the area of Alberta is occupied by lakes and uncultivated land.

Most significant was Carte's finding that patchiness of the hail pattern was a characteristic of all the storms he studied, from which he concluded that "the process of hail generation may be intermittent, even when it continues for several hours." (He also mentions receipt of the occasional report from most of the storms stating that the hail had come in several bursts - to be discussed later.) Figure 2 shows Carte's analysis of part of the 26 August 1959 hailswath, depicting both (a) the outline of the hail derived by his technique, and (b) shading representing maximum hail size.

2(v) Williams and Douglas

Williams and Douglas (1963) set out to investigate further the problem of hailswath continuity, adding the refinement of requesting from the observers reports of "no hail", an estimate of precision in their reported times, the most common size of hail, and qualitative information as to whether the point hailfall was continuous or intermittent.

Considering times, they concluded that it appears unlikely that a precision better than five minutes can be obtained, unless, of course, automatic recorders are used. We may note that, even if the observer does

his best in recording times, the accuracy of his timepiece in most cases is probably no better than plus or minus five minutes anyway. Door-to-door surveys, and telephone interviews, may add to the density of hail reports but not necessarily to the precision in time, since the observer is asked to recall times for storms which have taken place several hours or even days previously. Here the accuracy of the data is entirely dependent on the observer's memory. However, during 1965 and 1966, the telephone system and survey technique vastly improved so that lag time may be only a few hours.

In all a total of four 1962 Alberta storms were studied, for which the average data density was about 0.5 reports per square mile. Williams and Douglas note that, without exception, within the general boundaries of the swaths, demarcated by no-hail reports, all the farmers who were interviewed reported hail. They concluded from this that hail had fallen everywhere within the borders of the swaths. This finding therefore argues in favour of continuity in hailfall, which to Williams and Douglas suggested a hail-generation process without important spatial gaps. However, they admit the lack of sufficient evidence to state with any certainty whether the Alberta storms fit the "supercell" model of Browning and Ludlam (1960), or whether they consist of several individual cells which work together thus merely giving an impression of continuity.

Williams and Douglas point out the reluctance of farmers to report what to them appears to be "insignificant hail", and conclude that this "unreliability undoubtedly explains many of the 'holes' which Carte's analysis (which is highly sensitive to reliability) had revealed." In the light of more recent evidence, however, as discussed below, it now appears that the holes may be real.

2(vi) McBride

In 1963, McBride (1964) continued the practice of requesting "rain only" reports from Alberta observers; he also had the benefit of a 10-cm AN/FPS-502 radar with gray-scale which, although not calibrated, did provide qualitative shades of intensity to facilitate core-finding.

McBride studied in detail the major hailstorm which occurred on 14 July 1963, surveying a total area of 525 square miles, made up of western and eastern portions covering 225 square miles and 300 square miles respectively. A breakdown of the data sources for the two regions is provided in the Table below. In the west, 160 reports were received, representing a data density of

TABLE 2

Ground observer data for Alberta hailstorm of 14 July 1963
(McBride, 1964)

Number of Reports / Source*	Western Region (225 square miles)		Eastern Region (300 square miles)		Total	
	Hail	Rain	Hail	Rain	Hail	Rain
C	47	35	69	11	116	46
M	19	2	55	2	74	4
P	37	18	9	3	46	21
I	2	0	3	0	5	0
Subtotals	105	55	136	16	241	71
Totals	160		152		312	

*Note: The sources are C: car survey,
M: mailed-in cards,
P: telephone survey, and
I: Hail Insurance Board data.

0.7 reports per square mile, of which one third indicated rain only. The eastern area was slightly less densely populated, yielding 152 cards, which corresponds to 0.5 reports per square mile. Here 11% were rain-only reports. In all cases, the rain areas lay inside the envelope of the storm echoes, which was ample evidence to McBride of rain alone occurring within the hail-swath. This finding, which for the first time provided documented proof of the existence of hail-free areas, lends support to Carte's previous work (1963).

It would appear, therefore, that Williams and Douglas (1963) were either dealing with storms of a different nature, or simply failed to detect the hail-free areas in their survey. Perhaps it is significant that only about every second farmer in the observing network was interviewed*.

McBride concludes that "these rain areas are significant because they support the notion that this hailstorm was not a steady-state storm, consisting of a single cell with one large updraft which produced hail continuously. Indeed, the reports of interrupted hailfall, the radar evidence of many precipitation echoes within one storm, and the relationship of large hail to specific, short-lived echoes all support the same conclusion that this was not a steady-state storm".

2(vii) Pell

Further evidence of the multi-cellular nature of major Alberta hailstorms was provided a year later (Pell, 1965; 1966) when the "502" radar was improved to provide quantitative output with 10-db resolution such that

---

* Private communication from Dr. R.H. Douglas.

returned-power contours could be drawn for signals up to 60 db above noise level in intensity*. The severe storm which occurred on 18 July 1964 was singled out for an intensive study, from which Figure 3 is an excerpt. Shown are contours of the effective radar reflectivity factor, Z_e, for 1830 MST for each of the antenna's three tilt positions. The radar range at this time was 15 miles. The low, medium and high beams had vertical dimensions of 5, 7 and 9 degrees, respectively. Note that the low-beam picture depicts three distinct $Z_e = 10^5$ mm^6 m^{-3} radar cores, as well as ten lower-intensity "highs". The two southernmost 10^5 cores merge into one in the middle beam, and disappear in the high beam. However, the northern core changes little in the medium beam, but splits in two in the high-tilt picture.

2(viii) Carte

An analysis of a severe storm in South Africa on 15 January 1964 (Carte, 1964; 1966) showed a marked departure from a steady state of hail generation. This conclusion was based on variations of size of the largest and most common hailstones across and along the path, changes in the amount of hail and rain, changes in structure of the hailstones, and, most important, the finding of the hailfall to be multi-cellular in structure. The areas within which hail was falling at various times, positioned relative to a straight line representing the center of the hail path, are shown in Figure 4. According to Carte, the envelopes within which hail was falling

* This unit was taken out of service at the end of the 1964 hail season for purposes of modification. It was returned to the Alberta Hail Studies field site at RCAF Station Penhold in the spring of 1967 equipped with a high-resolution antenna (22-foot dish) and improved gray-scale display accessories.

at various instants were derived from the locations of observers (known to within a quarter of a mile) and from those times of hail onset and duration that were claimed to be correct within one minute. More than half the envelopes each enclose 20 or more data points, and in addition exclude negative reports.

In an attempt to match a standard mathematical contour to all the hail cells, Carte fitted to them an ellipse (see Figure 5) with major and minor axes of 12 miles and 5 miles, respectively, with an inclination to the hail path (spine) of 30 degrees, the ellipse having a mean speed of 29 miles per hour.

However, realizing the oversimplification of his model, Carte concluded that the Johannesburg-Pretoria hail path was laid down either from a number of separately acting convective cells, or from a single cell changing markedly with time, indicating the presence of a more complex airflow pattern than suggested by the study of the Wokingham storm.

2(ix) Browning and Fujita

In yet another study of severe local storms, this time in Oklahoma (Browning and Fujita, 1965), it was found in one specific case that even though the hailswath was continuous, it was in fact the product of a sequence of storm cells, "or of a non-steady storm, if you choose instead to define a storm as being the collection of cells". The authors do mention, however, that "some storms do attain a nearly steady-state for fairly long periods of time".

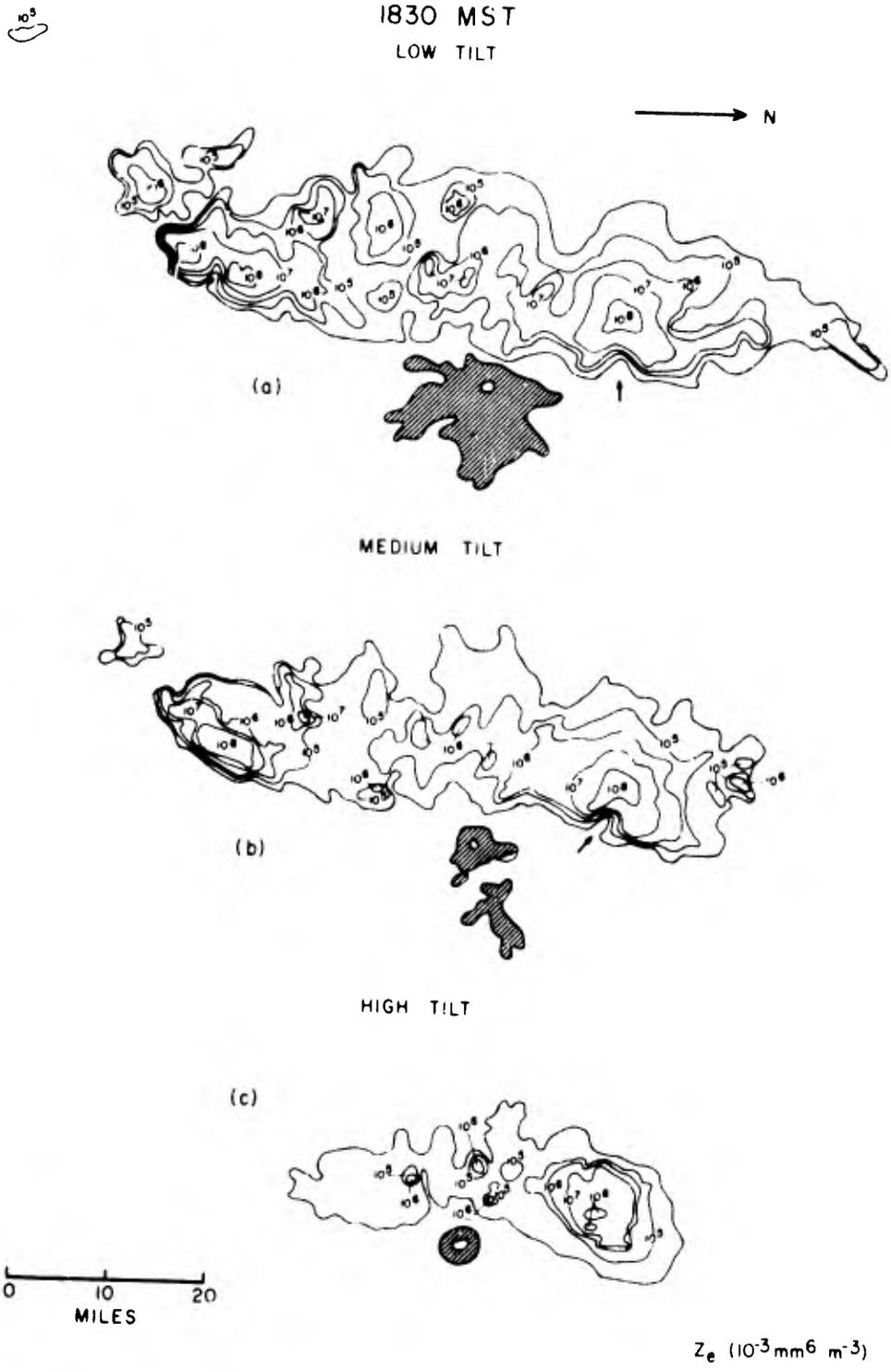

Fig. 3: Z_e isoecho contours for the Alberta hailstorm of 18 July 1964, 1830 MST. (a) Low beam only. (b) Medium beam only. (c) High beam only. Shaded areas are ground clutter. At this time, storm motion was due east. (Units for the contours are such that 105 on the chart signifies 10^2 mm^6 m^{-3}.)
Adapted from Pell (1965).

?(x) Douglas

The hailswath continuity problem for Alberta storms can best be summarized by a quotation from Douglas (1965):

> " It would appear that...Alberta hailstorms consist of a number of small active cells probably with short individual lifetimes, waxing and waning within an active area which itself retains an identity as it moves downswath. While there may be some instances of the 'steady-state' storm, as observed and discussed by Ludlam (1963) and others, the general impression is that Alberta hailstorms possess a remarkable degree of intermittency which seems more consistent with a cellular model than with a truly steady-state one."

In conclusion, a picture emerges on continuity in the Alberta hailswath as the exception, rather than as the rule. This correlates well with the multi-core structure which the radar generally observes in frontal thunderstorm systems. However, this is not to say that individual storm cells cannot attain a steady-state for relatively short durations (as compared to their total lifetimes). Indeed, segments of the swath may consist of continuous hailfalls produced by them. The Browning-Ludlam generator seems to be a special case; apparently we have here a single, very large storm cell which remains in a steady-state for an extra-ordinarily long time.

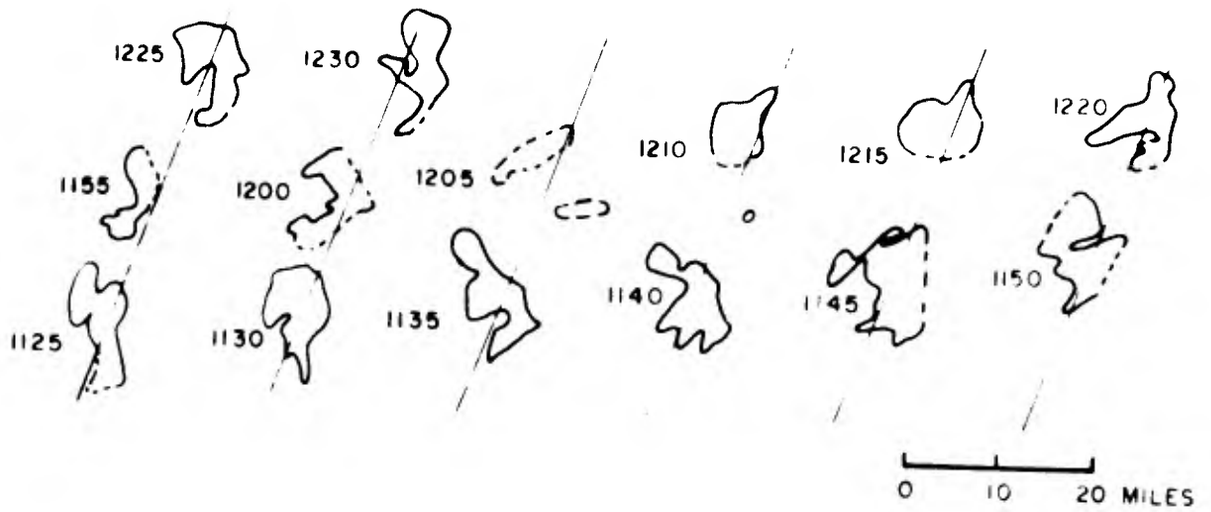

Fig. 4: An analysis of the severe South African storm of 15 January 1964, showing areas on which hail was falling at various times (GMT). Dotted lines indicate uncertainty in location of boundaries. Straight lines represent the center of the hail path. From Carte (1964, 1966).

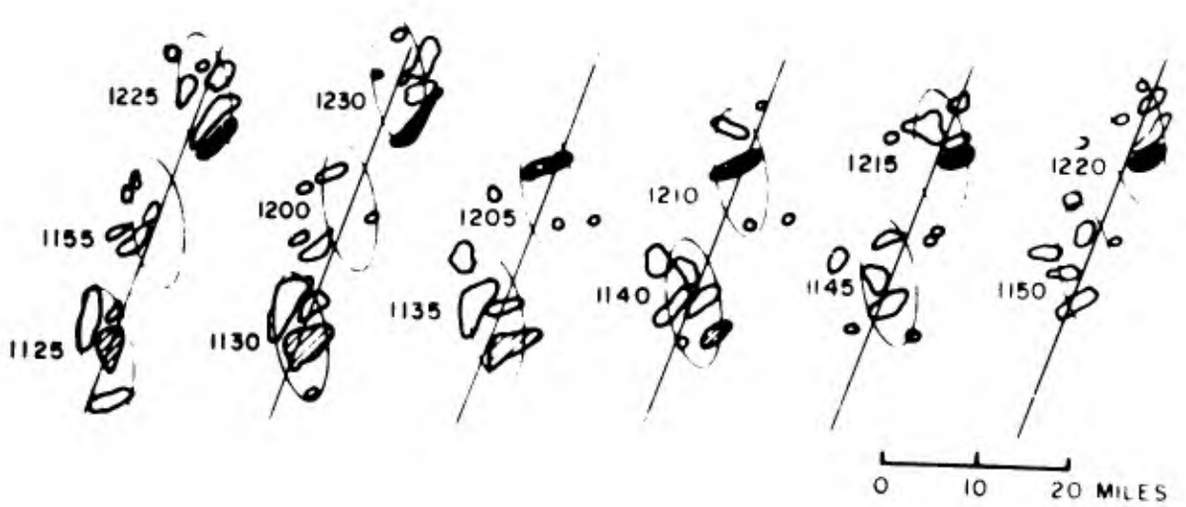

Fig. 5: Similar to Figure 4, with an ellipse fitted to the hail cells (see text). The two shaded cells show movement across the hail path. Straight lines are the same as in the previous figure.
From Carte (1964, 1966).

3. POINT HAILFALL CONTINUITY

Closely associated with the problem of continuity in the hailswath itself is the question of the nature of the point hailfall. It seems reasonable to expect that the steady-state "supercell" concept of Browning and Ludlam, if operative, would produce hail of like character at every point along the cell's trajectory. However, we shall show that this kind of swath is only one of several possibilities.

3(i) Changnon, Chmela, Schleusener and Auer

Changnon (1960), in a study of a severe Illinois storm, found that, on the basis of only 21 "reliable" observations, the average hail duration at a point was 12 minutes. Chmela (1960) found that for New England storms the median hail duration was about four minutes, although some reports of hail lasting up to 25 minutes were reeeived. A study of hailstorms in the high plains of the United States based on 1390 reports (Schleusener and Auer, 1964) showed that 25% indicated durations of 10 - 15 minutes, with 20% reporting durations longer than 20 minutes. Changnon and Stout (1962) found that the six hail cells they were able to construct (see Section 2(ii)) for a single storm were present for an average duration of 36 minutes, and that the average duration of hail cores within the cells, containing stones of diameter one inch or greater, was 28 minutes. However, none of these investigations provided any information regarding the continuous nature of the point-hailfalls throughout their durations.

3(ii) Carte

As mentioned earlier, Carte (1963) was the first to report that, in the twelve 1961 Alberta storms he studied, there were occasional receipts of volunteer information stating that the hail had come in several bursts. This opened the question of point continuity for further study.

3(iii) Williams and Douglas

A general question regarding whether the hailfall was continuous or intermittent was first asked of all Alberta observers in 1962. This led to the finding that hailfall was reported as intermittent in 50% of the cases, along with several notations of variations in intensity (Williams and Douglas, 1962). We may note that even continuous hailfall can vary in intensity, but this information was not requested at that time.

3(iv) McBride

McBride (1964), also working in Alberta, improved the question regarding point hailfall continuity by changing it from the 1962 form, "During this time hail was continuous____intermittent____," to "During this time: it hailed continually without much change in intensity____; it hailed more intensely at some times than others____; it stopped and started several times____." The result of his study was the finding that the percentage of reports of continuous hail decreases as the duration of hailfall increases. He also found this tendency regardless of how the intensity is reported to vary. Hailfalls of less than about 20 minutes duration have a continuity probability of at least 50%.

3(v) Douglas

Douglas (1965) points out that "reports of duration, together with the observed number of 'stops and starts', for all storms of 1963 suggest that the average duration of each individual burst within an interrupted point hailfall is of the order 4 - 7 minutes. If each burst is associated with an individual hail cell, moving at 30 miles per hour, then the average dimension along the direction of motion of such cells is of the order of 2 - 4 miles. These dimensions of 'cellular bursts' are substantially smaller than the active areas indicated by Carte (1963), but are comparable in size to the 'cells' discussed by Changnon and Stout (1962)".

3(vi) Carte

Carte (1964, 1966) working in South Africa, found, from 244 reports covering an area of 350 square miles for a specific storm, that the modal duration of continuous hail was 5 - 10 minutes, with a maximum of 35 minutes. In addition, he received "30 reports of intermittent hailfall from points scattered apparently at random all over the hailpath".

4. SUMMARY AND CONCLUSION

The above discussion shows that at least in many swaths hail-free areas definitely do occur. To go much beyond this point, it will be necessary to have reliable data obtained with good resolution in time (say, one minute) and in space (a network density of one observer per square mile or better). It is doubtful that this will be possible, in Alberta at least, with lay observers alone. Rather, one must face the task of designing automatic devices to supplement and aid, even calibrate - if not entirely to replace - the human observer.

Tables 3 and 4 are summaries of the contributions of the various authors discussed in this paper to the literature on hailswath and point-hailfall continuity, respectively. The references are listed in the order of mention in the text, which is approximately chronological.

TABLE 3

Summary of references to HAILSWATH CONTINUITY,
(in the order discussed in the text)

Author(s)	Year(s)	Contribution
Douglas and Hitschfeld	1958, 59	Persistent echo-top heights in Alberta presented as an argument for swath continuity.
Browning and Ludlam	1960, 62	Steady-state storm model - continuous-hail generator.
Ludlam	1963	
Browning	1965	
Hitschfeld and Douglas	1961	Observer evidence in Alberta of continuous-swath hailfall.
Douglas	1961, 63	Deficiencies in Alberta observer network.
Changnon and Stout	1962	Illinois continuous-swath hailfall may be due to overlapping from many hail cells.
Donaldson et al	1960	Strong biases in observers' reported times of hail onset and duration.
Douglas	1961	
Carte	1963	
Williams and Douglas	1963	
McBride	1964	
Carte	1966	
Schleusener and Henderson	1962	Separate hailfalls within a storm are of short average duration.
Carte	1963	Evidence of swath intermittency in 12 Alberta hailstorms.
Williams and Douglas	1963	Evidence of hailswath continuity in Alberta storms.
McBride	1964	First documented proof of hail-free areas in an Alberta storm.
Pell	1965, 66	Radar evidence of multi-cellular structure of major Alberta hailstorms.
Carte	1964, 66	Multi-cellular hailfall in a South Africa storm.
Browning and Fujita	1965	Continuous hailswath in an Oklahoma storm produced by a sequence of storm cells.
Douglas	1965	Alberta hailstorms "consist of a number of small active cells" and "possess a remarkable degree of intermittency."
Pell	This article	A picture emerges of continuity in the Alberta hailswath as the exception, rather than as the rule.

TABLE 4

Summary of references to POINT-HAILFALL CONTINUITY,
(in the order discussed in the text)

Author(s)	Year(s)	Contribution
Changnon	1960	Average point hail duration is 12 minutes in an Illinois storm.
Chmela	1960	Median hail duration in New England storms is about 4 minutes.
Schleusener and Auer	1964	Point hailfall in United States high plains usually lasts less than 20 min.
Changnon and Stout	1962	Average duration of six Illinois hail cells is 36 minutes.
Carte	1963	First to note reports of intermittent point-hailfall in Alberta.
Williams and Douglas	1962	Intermittent point hailfall in 50% of Alberta reports.
McBride	1964	Percentage of continuous-hail reports decrease as duration increases (Alberta).
Douglas	1965	Average duration of each individual burst in Alberta intermittent point-hailfall is 4 to 7 minutes.
Carte	1964, 66	Modal duration of South Africa continuous hail is 5 to 10 minutes, with maximum of 35 minutes. Also noted intermittency.

REFERENCES

Browning, K.A., 1962: Air flow in convective storms. Quart. J.R. Meteor. Soc., 88, 117-135.

——— and T. Fujita, 1965: A family outbreak of severe local storms - a comprehensive study of the storms in Oklahoma on 26 May 1963, Part 1. Air Force Cambridge Research Labs., Special Reports, No. 32, Office of Aerospace Research, United States Air Force.

——— and F.H. Ludlam, 1960: Radar analysis of a hailstorm. Technical (Scientific) Note No. 5, Contract No. AF 61 (052)-254, Dept. of Meteor., Imperial College of Science and Technology, London.

Ca te, A.E., 1963: Some characteristics of Alberta hailstorms. Sci. Report MW-36, Stormy Weather Group, McGill University, Montreal.

———, 1964: Hailstorms in Johannesburg, Pretoria and surroundings on January 15 and 16, 1964. Council for Scientific and Industrial Research Report 228, Pretoria, South Africa.

———, 1966: Features of transvaal hailstorms. Quart. J.R. Meteor. Soc., 92, 290-296.

Changnon, S.A. Jr., 1960: A detailed study of a severe Illinois hailstorm on June 22, 1960. CHIAA Research Report No. 6, Illinois State Water Survey, Urbana, Illinois.

——— and G.E. Stout, 1962: Details of surface characteristics displayed by Illinois hailstorms. Illinois State Water Survey. Presented at Severe Storms Conference, Amer. Meteor. Soc., Norman, Oklahoma, 13 - 15 Feb. 1962.

Chmela, A.C., 1960: Hail occurrence in New England: some relationships to radar echo patterns. Proc. Eighth Weather Radar Conference, San Francisco, California.

Donaldson, R.J., Chmela, A.C., and C.R. Shackford, 1960: Some behaviour patterns of New England hailstorms. Amer. Geophys. Union, Monograph 5, Physics of Precipitation, 354-368.

Douglas, R.H., 1961: The study of an Alberta hailstorm. Sci. Report MW-35, Stormy Weather Group, McGill University, Montreal.

———, 1963: Recent hail research: a review. Severe Local Storms, Meteor. Monogr., Vol. 5, No. 27, Boston, Amer. Meteor. Soc.

Douglas, R.H., 1965: Intermittency in Western Canadian hailfall. Proc. Inter. Conf. on Cloud Physics, May 24 - June 1, 1965, Tokyo and Sapporo, Japan.

——— and W. Hitschfeld, 1958: Studies of Alberta hailstorms, 1957. Sci. Report MW-27, Stormy Weather Group, McGill University, Montreal.

———, and ———, 1959: Patterns of hailstorms in Alberta. Quart. J.R. Meteor. Soc., 85, 105-119.

Hitschfeld, W., and R.H. Douglas, 1961: A theory of hail growth. Sci. Report MW-35, Stormy Weather Group, McGill University, Montreal.

———, and ——, 1963: A theory of hail growth based on studies of Alberta storms. Zeitschrift für angewandte Mathematik und Physik (ZAMP), 14, 554-562.

Ludlam, F.H., 1963: Severe local storms: a review. Severe Local Storms, Meteor. Monogr., Vol. 5, No. 27, Amer. Meteor. Soc., Boston.

McBride, J.H., 1964: Small-scale structure of hail swaths. M.Sc. thesis, Dept. of Meteor., McGill University, Montreal.*

Pell, J., 1965: A quantitative hailstorm study using broad vertical-beam radar. M.Sc. thesis, Dept. of Meteor., McGill University, Montreal.*

———, 1966: Quantitative hailstorm studies using broad vertical-beam radar. Proc. Twelfth Conference on Radar Meteorology, Norman, Oklahoma, Oct. 17 - 20, 1966, Amer. Meteor. Soc., Boston.

Schleusener, R.A., and A.H. Auer Jr., 1964: Hailstorms in the High Plains. Final report, NSF Grant G-23706, Civil Engr. Section, Colorado State University, Fort Collins, Colorado.

_____, and T.J. Henderson, 1962: Observational data on the position of hail-fall with respect to precipitation cells. Atm. Sci. Tech. Paper No. 25, Civil Engr. Section, Colorado State University, Fort Collins, Colorado.

Williams, G.N. and R.H. Douglas, 1963: Continuity of hail production in Alberta storms. Sci. Report MW-36, Stormy Weather Group, McGill University, Montreal.

---

* Both these theses are due to appear shortly in abbreviated form in this series of Scientific Reports.

SMALL SCALE RADAR STRUCTURE OF ALBERTA HAILSTORMS

by

A.J. Chisholm

CONTENTS

SMALL SCALE RADAR STRUCTURE OF ALBERTA HAILSTORMS

A.J. Chisholm

ABSTRACT

A study of radar echo maxima in two Alberta hailstorms has shown that the storms consisted of several storm "families", each containing small intense radar echo "cores" or cells. These cells developed preferentially on the right flank of the family, moving across the track of the family at an acute angle to dissipate near the left flank; identifiable lifetimes of the cells were 20-30 minutes. There appeared to be a cycle of development of the cells, which had a considerable effect on the overall storm-family velocity.

1. INTRODUCTION

The study of motion and development of severe convective storms by radar requires data with high resolution in both time and space. In addition, sufficient detail about the storm structure must be available in order to identify a given element at the time of the following radar sequence. This permits one to distinguish between motion and development. Acquisition of 10 cm radar data with grey-scale intensity contours at 5 db intervals (from 0 to 60 db) and a cycle time of 3 min prompted a study of the small-scale radar structure of two Alberta hailstorms. Initial echo locations were determined and related to the storm center and the local geography. As well, the subsequent motion and development of these echoes were studied to determine lifetimes, directions of travel and the relations between adjoining echoes.

2. DATA

The radar data for this study were obtained by an AN/FPS-502 radar unit operated by the Alberta Hail Studies Project at Penhold, Alberta, during the summer of 1964. Characteristics of this radar are listed in Table 1. A grey-scale stepping circuit similar to the one used by the Stormy Weather Group at Montreal was used to display intensity contours of P_r (returned power) at 5 db intervals on the PPI scope. Five shades of grey were used, but successive gain reductions of 20 db and 40 db supplied additional data so that intensity contours of P_r (returned power) from 0 to 60 db were available. The PPI display was photographed on Kodak 35 mm TRI-X film. In order that the radar film data could be used for quantitative purposes densitometry tests were performed in the field, and the radar settings and darkroom techniques rigidly controlled. Although the maximum operating range of the radar was 80 n mi, only echoes which occurred between 20 and 60 n mi were studied. The resolution of the radar data was therefore of the order of 1 n mi or better. As complete radar data were available at 3 min intervals, the spatial resolution of 1 n mi is therefore comparable to the distance which the storm would move in 3 min.

TABLE 1

AN/FPS-502 radar parameters

P_r	(minimum detectable power)	10^{-13} w
P_t	(transmitted power)	300 kw
h	(pulse length)	540 m
λ	(wavelength)	10.6 cm
θ	(horizontal half-power beam width)	1.2°
ϕ	(vertical half-power beam width)	5.0°
f	(microwave radiation frequency)	2835 Mcps
A_p	(effective apertural antenna area)	9.75 m^2
PRF	(pulse repetition frequency)	480 pps
Ω	(antenna rotation rate)	5 rpm

3. THE SYNOPTIC WEATHER PATTERN

The hailstorms studied occurred on 18 July and 21 July 1964. Circulation patterns for these two days show striking similarities at both surface and upper levels. An upper cold trough was located over southwestern British Columbia with an upper warm ridge centered over Saskatchewan. A jet stream extending northeastward from Washington through central Alberta and eastward into Saskatchewan and Manitoba was oriented southwest-northeast over the project area. The winds at 300 mb were in excess of 100 kts with the highest wind shear values occurring between 10,000 and 30,000 ft. The storms were associated with jet stream maxima and were found near the "right entrance" or "left exit" regions where upper level divergence is known to be a maximum. A study by Proppe (1965) on the association of jet stream maxima

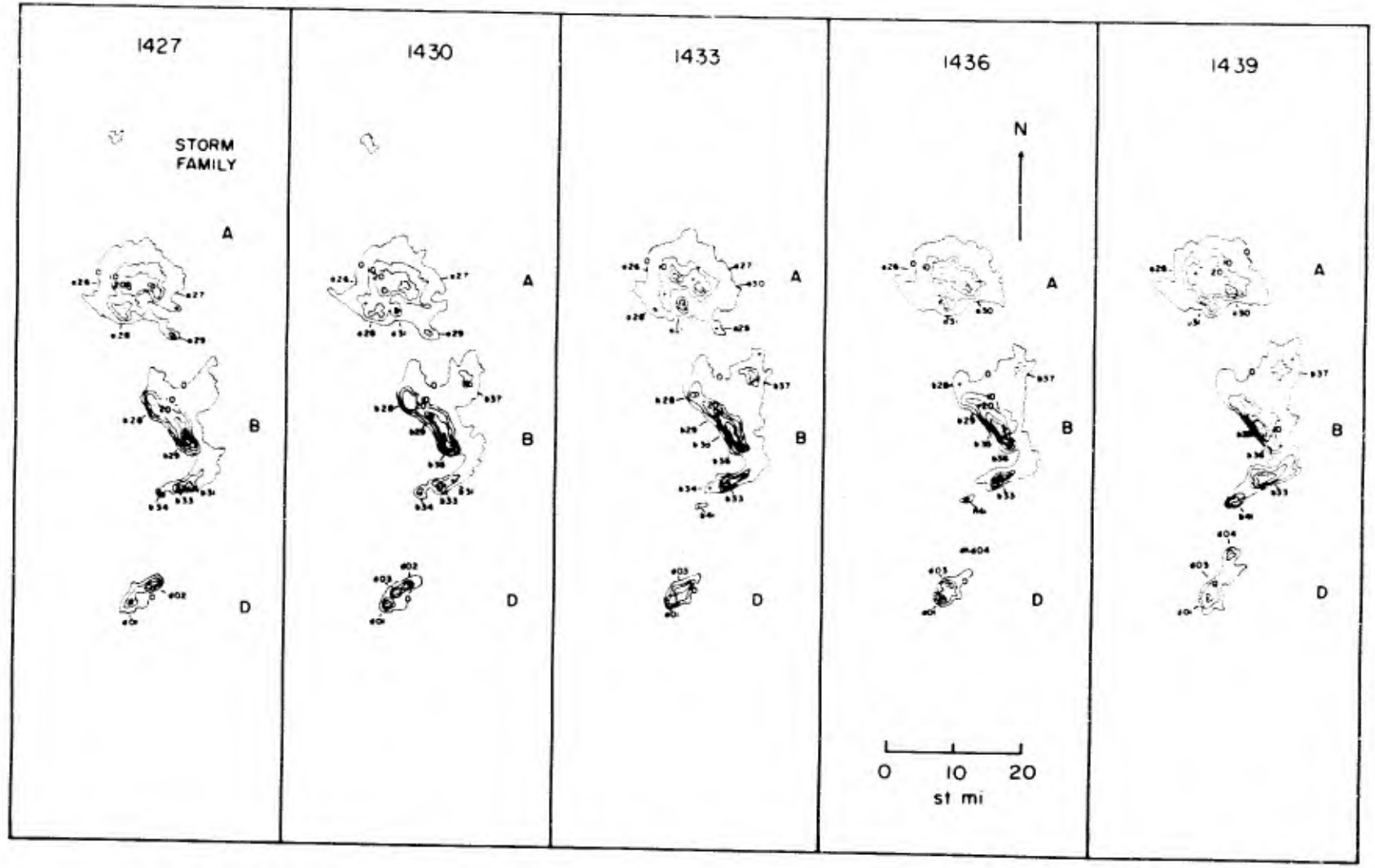

Fig. 1: Storm of 21 July 1964. Contours of P_r, in steps of 10 db (up to 60 db), are shown at three-minute intervals. Individual cells are labelled a26, a27 etc. for family A; b29, b30 etc. for family B. Note southward development of family D.

and hailstorm occurrence in Alberta also revealed a relation between jet stream maxima and hail occurrence. Proppe was able to show that the proximity of a jet axis is not in itself a factor which enhances hail activity; on the other hand his analysis of the position of jet stream "entrance" and "exit" regions showed that the "left exit" region was a favored area for hailstorm activity.

The surface synoptic maps for 18 and 21 July show a lee trough lying in a north-south line through the project area. This synoptic pattern would contribute to low-level convergence and in addition help to increase the low-level moisture supply throughout central Alberta.

A study of the radiosonde data available from Edmonton and Calgary (approximately 100 mi north and south of Penhold, respectively) at 0500 and 1700 MST (Mountain Standard Time) revealed that the airmasses associated with these two storms were indeed unstable. A complete stability analysis was impossible, however, due to the times of radiosonde release and storm passage. It was therefore not possible to estimate convective cloud tops with any degree of confidence.

On both days showers and thunderstorms were initiated in the foothills region west of Penhold by weak eastward-moving cold fronts. The two hailstorms studied by radar were found associated with these cold fronts.

4. ANALYSIS OF THE RADAR DATA

The radar data were analyzed at 3 min intervals for the purpose of studying the initiation, development and motions of radar echo maxima. This was accomplished by tracking the echoes relative to the earth and also relative to the storm centre itself. During the analysis it was found that the radar echo maxima were "cells" approximately 1-4 mi in diameter. It was apparent that these cells were the basis for large "storm families" or "clusters" (approximately 5 mi x 15 mi) of cells in a constant process of formation, growth and dissipation. With intensity contours from 0-60 db, the interior structure of these storms could be analyzed so that it was possible to follow the motion of individual cells within a storm family with some degree of confidence. The majority of the radar echo maxima which existed in these storms were found in families, so the data presented here will concentrate on the radar structure of these storm families.

5. RESULTS

Both storms were first detected about 60 n mi west of the radar site travelling eastward at approximately 30 kts. Each hailstorm was found to be composed of a family of cells with a consistent pattern of organization displayed in its overall structure. As these storm families developed and moved eastward new cells formed in preferred areas with a resulting characteristic linear structure and pattern of motion. Figure 1 illustrates a typical sequence of events for the period 1427 to 1439 MST. During this

period the storm was composed of three families A, B and D. New echo formation (such as echoes a31, b36 and b41) occurred on the right flank of the particular storm family. Also shown is the progressive southward development of the total storm as is indicated by the growth of storm family D.

Fig. 2 shows the track followed by the storm, as an entity, and also the tracks of a number of individual high-intensity radar cells. The individual cells are seen to move across the storm-track at a sharp angle, from southwest to northeast. Such behaviour has been observed by Browning (1965) in a severe storm family in Oklahoma. Browning's explanation for such behaviour is that the northernmost storms are cut off from their supply of warm moist low-level air, whereas the southernmost storms develop due to a ready source of warm moist air.

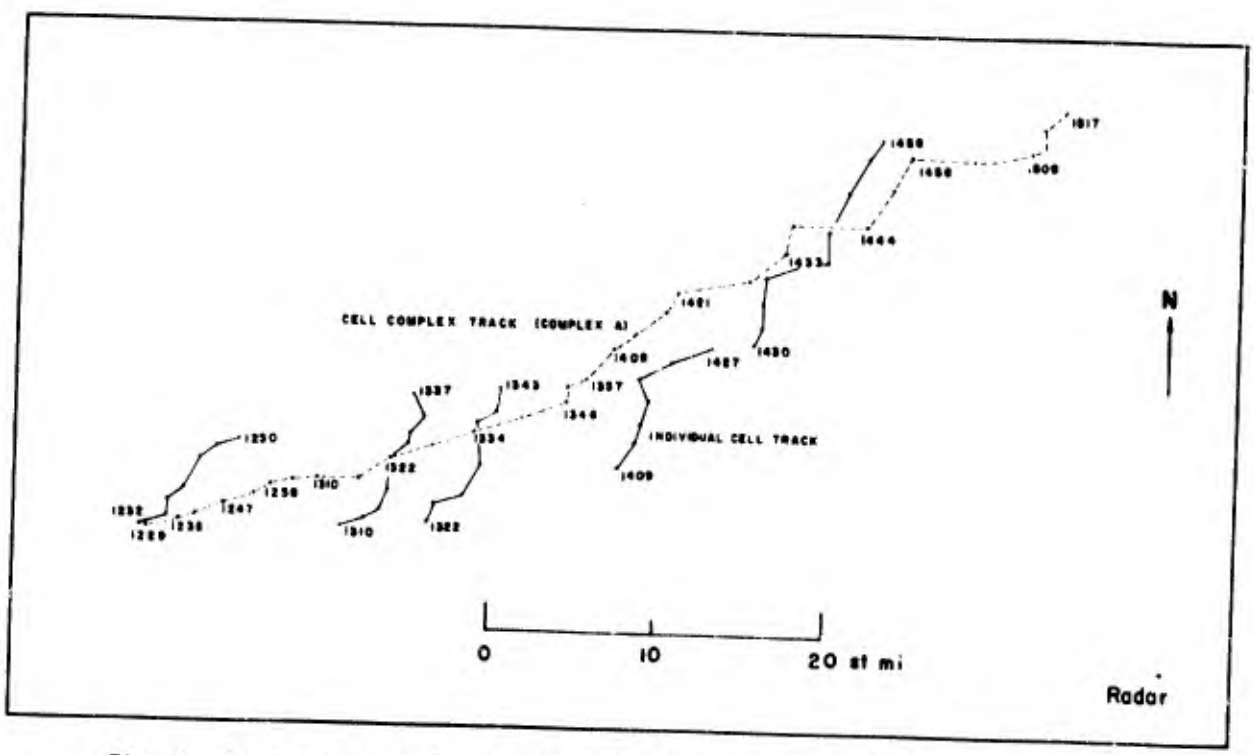

Fig. 2: Storm centre track and individual cell tracks for the storm of 21 July 1964. The dashed line shows the motion of the centre of storm complex A, at six-minute intervals. Solid lines show the motions of individual cells at three-minute intervals. Only about one-seventh of the total number of cell tracks are shown.

As data for the initial location of echoes were available, the relation of these points to local topography was examined. However, no obvious relationship between topography and initial echo location was found even though allowance was made for the fact that the first echo location might occur some time after the initial appearance of cloud. Instead, the initial appearance of radar echoes was found to occur with considerable frequency and regularity on the right flank of an existing storm family.

The length of time which an individual radar cell exists as a recognizable radar maximum is of considerable interest since it gives an insight into the time scale of a hailstorm and may also offer clues to help solve the problem of hailstone growth. Although the storm families were found to exist for periods of two or more hours, individual cells (i.e. recognizable echo maxima) were found to be much shorter-lived. Figure 3 shows the percent frequency of radar echo durations for the storms of 18 and 21 July 1964. The histogram for 18 July shows that 92% of all echoes studied had durations between 5 and 25 min. Similarly, in the 21 July storm, 86% of the echoes had durations between 10 and 30 min. Battan (1953) in a study of Ohio storms using a 10 cm radar found similar durations. However it should be pointed out that Battan's findings are for storms which remained as single cells, whereas the data presented in this study are for multi-cellular storms. It should be noted that the terms "lifetime" or "duration" refer to the period during which a recognisable radar maximum existed.

The lifetimes of these radar echo maxima imply that the growth of hail occurring in such cells must be rapid, occurring in the course of 20-30 minutes or less. Hitschfeld and Douglas (1963) have also found that

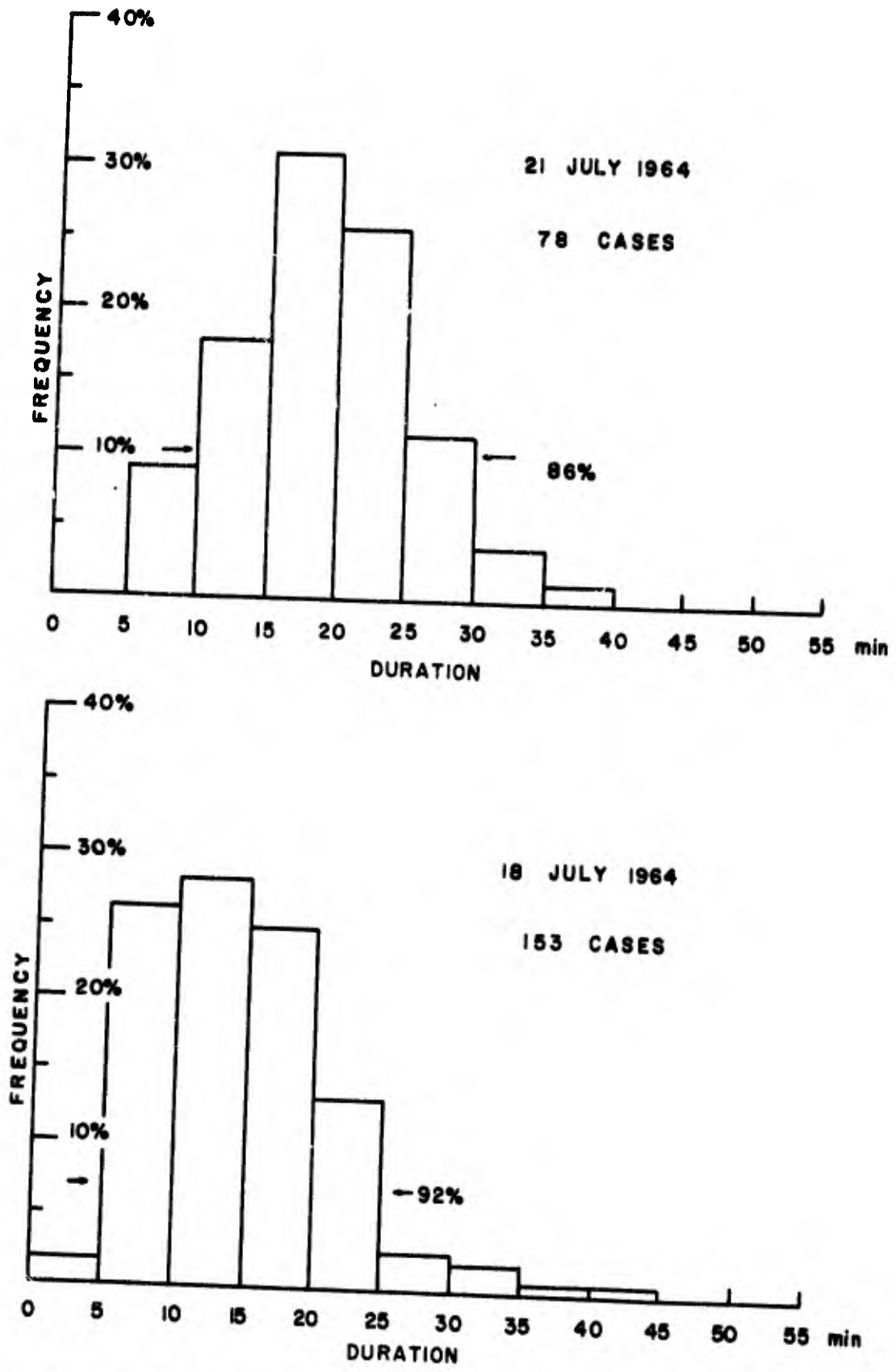

Fig. 3: Histograms of the radar duration of echo maxima. Range between arrows in upper diagram contains 86% of the cases; in lower diagram 92%.

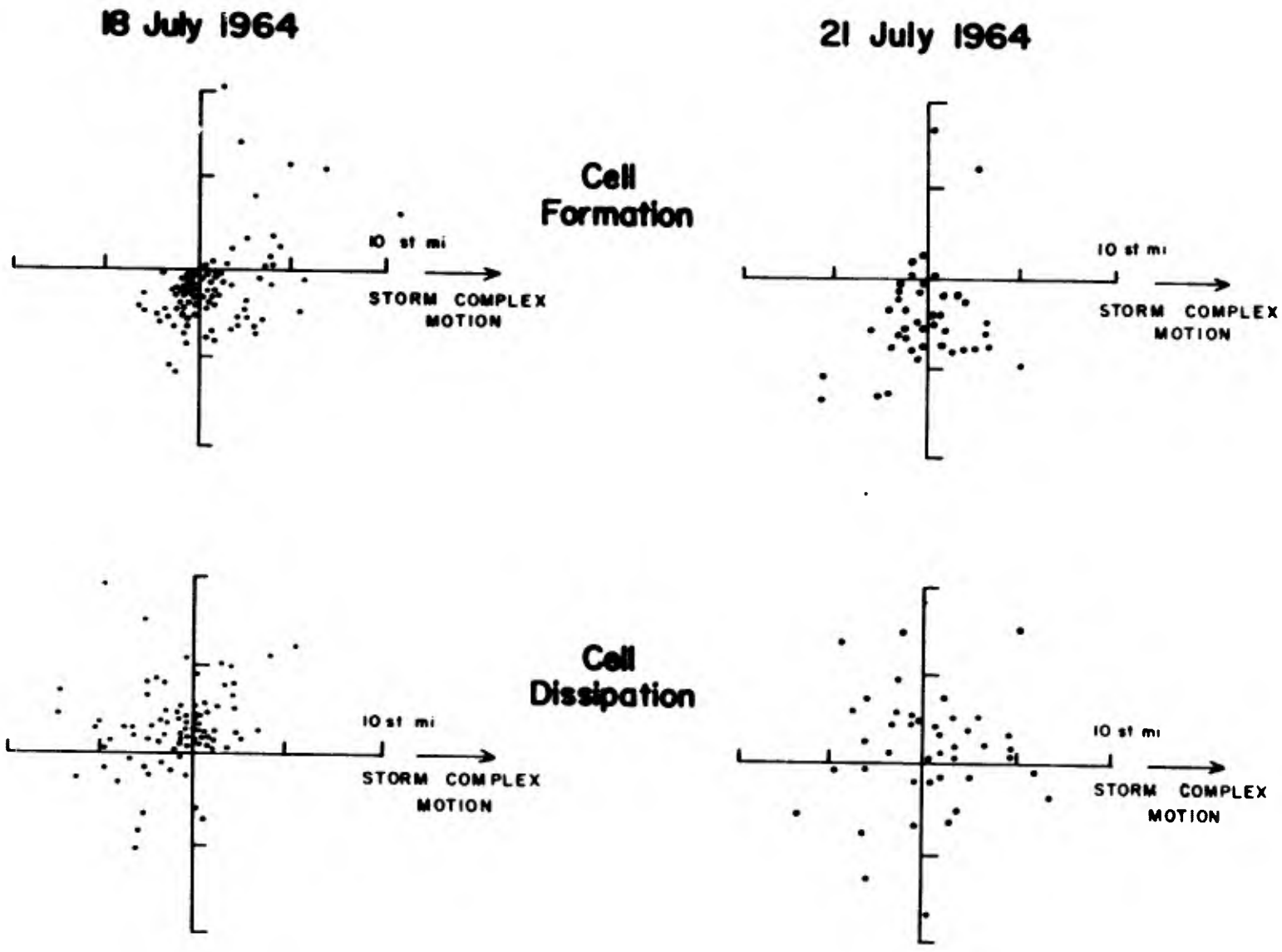

Figures 4 (left column) and 5 showing the location (relative to the centre of the complex) where cells formed and dissipated in the storms of 18 and 21 July 1964.

the elapsed time between the first radar evidence of a storm and the first hail reported at the ground might typically be 25 minutes.

The lifetime of a given cell, as observed by radar, is dependent upon such factors as the size, range and reflectivity of the cell, the background against which the maximum is compared, and the sensitivity of the radar unit itself. A complete study of cell lifetimes should include all these factors. Nevertheless, although the two histograms show lifetimes from widely differing cells, it is quite evident that radar cell lifetimes are of the order of 20 minutes.

During the analysis of the storm motions, individual cells were tracked relative to the ground and also relative to their storm family centre. The latter procedure was accomplished by defining the storm centre to be the centre of gravity of the intense portion of the storm family. Thus it was possible to determine the location of echo formation and dissipation with respect to the storm family centre. Figures 4 and 5 illustrate the location of echo formation relative to the storm family centre. The major portion of these points fall to the right of the storm centre. The area of most concentrated cell formation in the storm of 18 July was the right rear flank. A less common mode of echo formation was also found. This was the type of echo which forms along the leading edge of the storm family and rapidly becomes the main centre of activity. After formation the cells were found to grow in size and intensity while migrating northward through the storm family. Figures 4 and 5 also show the cells to have dissipated on the left side of the storm centre, indicating this northward movement through the storm and showing the dissipation on the northern storm boundary.

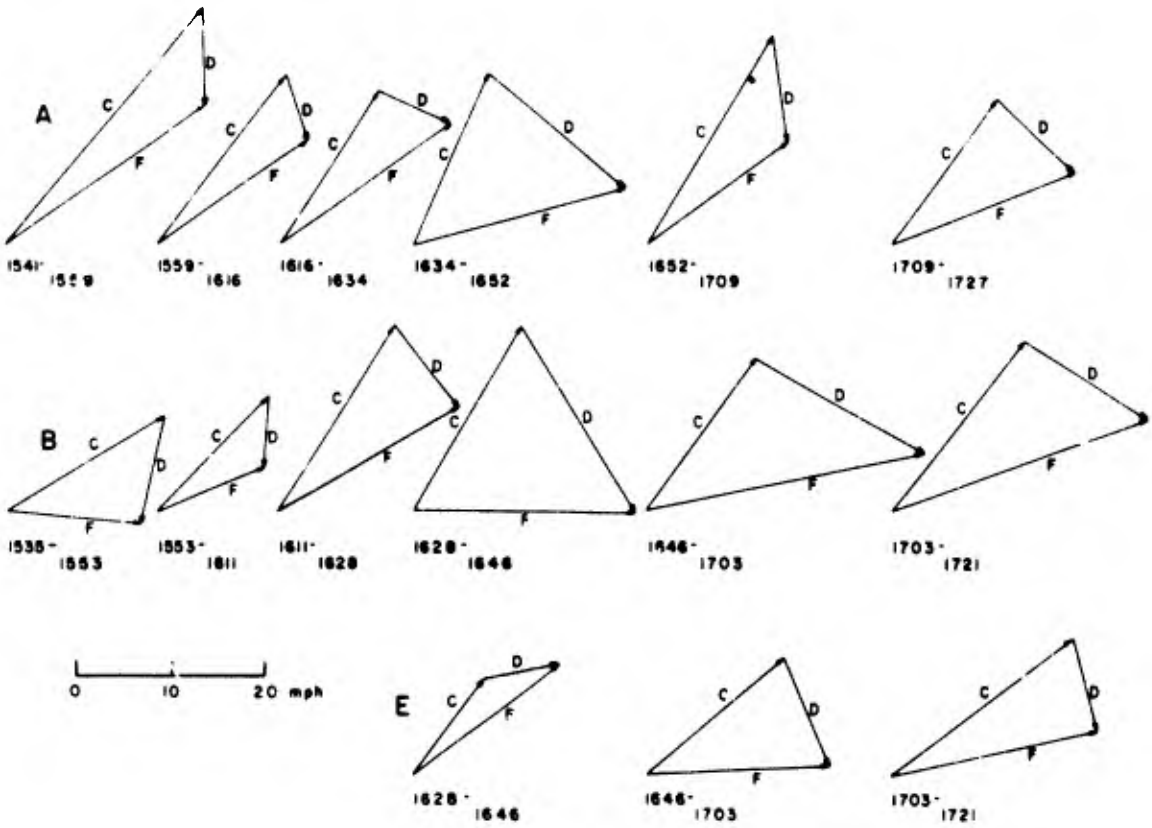

Fig. 7 (above): Velocity vector diagrams for the storm of 18 July 1964. Vector diagrams of the cell velocity (C), family velocity (F) and development velocity (D) are illustrated for families A and B. Times shown are Mountain Standard Time.

Fig. 8 (below): Velocity vector diagrams for the storm of 21 July 1964. Vector diagrams of the cell velocity (C), family velocity (F) and development velocity (D) are illustrated for families A and B. Times shown are Mountain Standard Time.

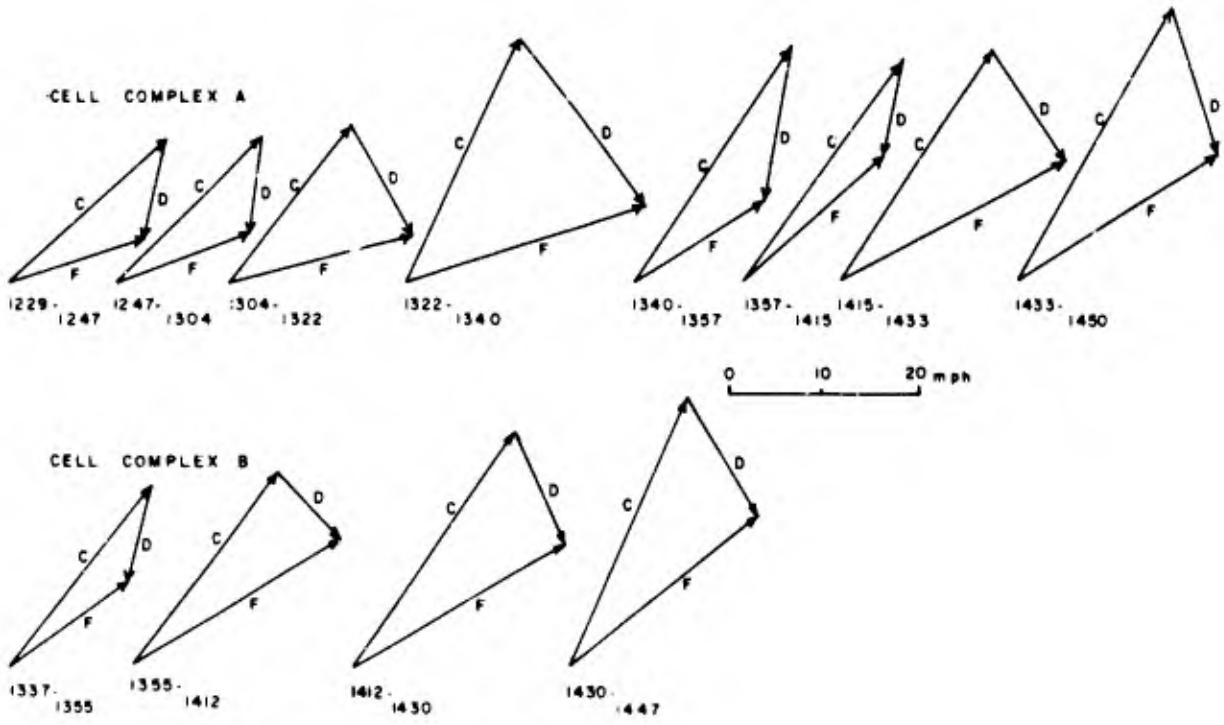

It is quite clear that the mechanism of preferential development on the right flank of a storm family results in the storm family having a different speed and direction of motion than the individual cells within it. The storm families studied were found to move to the right of the cells. This type of behaviour has also been observed by Newton and Fankhauser (1964) in storms on the Great Plains. Newton and Fankhauser found a correlation between the angle of departure and the size of the storm and postulated a model for the water budget as an explanation of this behaviour.

No obvious relation between the size and the angle of departure was indicated in the storms of 18 and 21 July and so a correlation between these two parameters was not attempted. The deviation of large storms to the right of the motion of individual cells is readily accounted for by the preferential formation of new cells on the right hand flank and their subsequent motion across the storm path.

In an attempt to summarize and illustrate the cell motions, family motion and the development of a storm, a series of vector averages have been calculated and are shown in Figs. 7 and 8. Figure 6 is a schematic diagram which relates the vectors to the actual storm and the paths taken by the cells and the storm family. It also illustrates the angular departure of the cell tracks from the family track and points out the

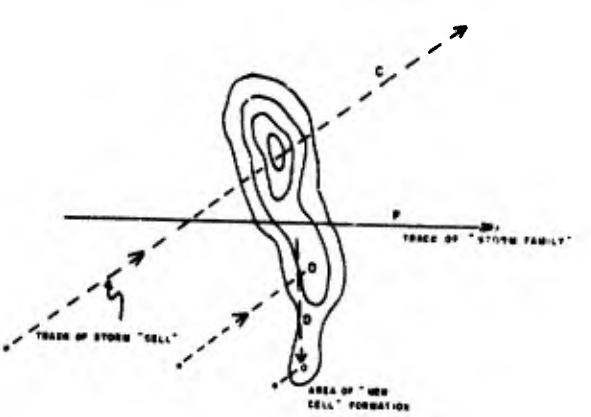

Fig. 6: Schematic of storm family, showing directions of motion of family and of cells. New cells, forming to the right of the family-centre, move diagonally across the path of the family. The vectors F and C indicate the velocities of the family and of the cells, respectively; vector D, the difference between F and C, is considered a development vector.

relative location of new cell formation. The average velocity of the individual cells in a particular storm family over an 18 min period is given by the C (cell) vector. The F (family) vector represents the average velocity of the storm family centre during the same time period. The difference vector, indicating the development of the storm family over the same 18 min period, is labelled D (development).

Study of these vector series reveals several interesting points. In figure 8, it can be seen that the C vectors for the storm families A and B are remarkably similar, with an average vector difference of approximately 4 mph which is of the order expected from the measurement technique. Further the C vectors for both storms (Figs. 7 and 8) are also quite similar. This is the type of behaviour which one might expect from a cellular storm embedded in a uniform environmental wind. An attempt was made to relate the cell velocities with the known wind structure (Chisholm, 1966). The wind data available were for Edmonton and Calgary, each approximately 100 miles from the radar site, north and south, respectively. Another difficulty was that the great vertical depth of the radar beam did not permit adequate resolution in the vertical for a good comparison between echoes and winds. Still, surprisingly good agreement was found between the cell velocities and winds averaged between the 4000 and 20,000 ft levels which are the limits of the radar field of view.

On the other hand the F vector varied considerably during the same period. This is best illustrated by the behaviour of the D vector which is the difference between the C and F vectors. In both cases the D vector, which is initially small in magnitude, begins by pointing to the right rear flank of the storm centre. As time progresses, the D vector increases in magnitude and

rotates anticlockwise. The mature stages of Complex B could not be analyzed but in the case of Complex A the D vector reversed its behaviour, decreasing in magnitude and rotating clockwise back to its original orientation. A second cycle appears to have been beginning as the storm passed out of radar range.

The similarities in the vector diagrams for the storm of 18 July (figure 7) are striking. All three families show the same form of cycle for the D vector which increases in magnitude while turning anticlockwise; it then swings back clockwise while decreasing in magnitude. The C vectors show the same behaviour exhibited in the other storm although there is a consistent variation believed to be due to the north-south structure of the jet stream.

6. CONCLUSIONS

A study of radar echo maxima from two Alberta hailstorms in similar synoptic situations has revealed storms which consisted of several storm families, each composed of small cellular echoes. The storms were found to exist in a highly sheared environment near areas of maximum upper level divergence associated with jet stream maxima. The radar echoes showed a definite preference in forming on the right (south) flank of an existing storm family. They proceeded to move northward through the storm family with radar durations of 20-30 minutes. A study of the motions of individual cells reveals a cycle of development which has considerable effect on the overall velocity of the storm family.

REFERENCES

Battan, L.J., 1953: Duration of convective radar cloud units. Bull. Amer. Meteor. Soc. 34, 227-228.

Browning, K.A., and T. Fujita, 1965: A family outbreak of severe local storms - a comprehensive study of the storms in Oklahoma on 26 May 1963, Part 1. AFCRL-65-695(1). Special Report No. 32, 346 pp.

Chisholm, A.J., 1966: Small scale radar structure of Alberta hailstorms. M.Sc. Thesis, McGill University, Dept. of Meteorology, April 1966.

Hitschfeld, W., and R.H. Douglas, 1963: A theory of hail growth based on studies of Alberta storms. ZAMP (J. Appl. Math. and Phys.) 14, 554-562.

Newton, C.W., and J.C. Fankhauser, 1964: On the movements of convective storms, with emphasis on size discrimination in relation to water-budget requirements. J. Appl. Meteor. 3, 651-668.

Proppe, H.W., 1965: The influence of wind shear on Alberta hailstorm activity. M.Sc. Thesis, McGill University, Dept. of Meteorology, April 1965.

ON THE TEMPERATURE OF HAILSTONES

by

Marianne English and Walter Hitschfeld

The following three pages contain corrections for an arithmetical error in the contribution "On the temperature of hailstones", which was contained in Report MW-42, July 1965.

TABLE 1.

1 Hail Trajectory Number	1	2	3	4	5	6	7	8	9
2 Maximum updraft (m sec^{-1})	15	15	15	17.5	17.5	15	15	15	17.5
3 Stored rain concentration (g m^{-3})	30	20	10	30	10	10	20	30	20
4 Temperature at which embryo starts growth (°C)	-10	-10	- 5	-10	- 5	-10	-15	-15	-10
5 Top of trajectory (km)	5.0	5.0	4.2	5.2	4.8	6.3	7.6	7.5	6.7
6 Hail diameters where fraction liquid is 60% (cm)	1.0	1.5	1.5	1.8	2.5	3.5	4.5	5.0	5.5
7 Height above surface where fraction liquid is 60% (km)	5.0	4.9	3.8	4.8	4.3	4.1	4.4	4.5	4.4
8 Time for particle to reach freezing level (min)	6	7	10	6	13	20	26	25	20

TABLE 2.

Liquid fraction (%) of stone:									
9 When passing 0-C level (2.67 km)	3	34	52	42	54 (0)	57 (0)	58 (23)	58 (31)	58 (38)
10 At ground, where temperature of air is 14C.	36	50	68	54	61 (0)	61 (0)	60 (22)	60 (30)	60 (37)

These Tables are copied from p. 58 of Report MW-42, with corrected entries shown in rows 9 and 10. (Items in brackets are the old erroneous results.)

Table 1 contains information about hailstones growing according to the Hitschfeld-Douglas theory proposed in Report MW-35, and was originally presented there. In the model situation assumed, the hail acquires a rather high water content, and rows 6 and 7 indicate size and height where the liquid fraction is 60%. Assuming that the stones are ejected from the cloud in this condition, rows 9 and 10 indicate the liquid fraction the stone would have, when passing the freezing level, and when arriving at the surface.

ON THE TEMPERATURE OF HAILSTONES

a correction

Marianne English and Walter Hitschfeld

In Table 2 of the article under the above title which appeared on p. 58 of Report MW-42, Hitschfeld and Stauder presented results of calculations concerning the progressive freezing of large wet hailstones chiefly by evaporation, if they fall clear of the cloud. A recent re-examination of the problem has revealed serious arithmetical errors in the older work. For comparison, both sets of results are shown in Table 2, opposite, with the previously quoted results shown in brackets. (Table 1, on which both calculations are based, is shown for reference.)

The new results show quite clearly that above the freezing level the evaporative cooling is much less effective than had been thought, and that no appreciable freezing results, except for the smaller stones. Thus stone No. 1, which is 1.0 cm in diameter when it leaves the cloud at a height 5.0 km while containing 60% water, only contains 3% water when it passes the 0-C isotherm; it contains 36% water when arriving at the surface. The larger stones also dry out a little above the freezing level, but all contain 50% or more liquid by the time they reach the surface. These results indicate that simple ejection from the cloud is not likely substantially to solidify the very wet hailstones resulting from the Hitschfeld and Douglas model of hail trajectories, as described by them in Report MW-35.

Both the present and the earlier calculations apply to a hailstone ejected from the cloud into clear air of relative humidity 66%. As already mentioned, at the moment of its ejection, the stone is considered to contain 60% liquid water by weight. Both now and earlier, the simple assumption is made that a partially liquid stone has a uniform temperature of 0C. This may well be unrealistic at air temperatures colder than 0C. In that case, the outer layers of the stone are likely to freeze, causing its surface temperature to approach that of the air, while the centre of the stone remains an ice/water mixture at a temperature of 0C. Heat transfer between air and stone is then reduced, since any latent heat released must be conducted through the ice before it is transferred to the air. In reality, then, the heat transfer from the stone to the air is likely to be less efficient than predicted by the uniform-temperature model. Nevertheless this model gives an indication of the maximum cooling that can be expected.

In connection with this new calculation, no fault was found with the theory, as described in Appendix 4 (pp 68,69) of our Report MW-42. But this opportunity is taken to correct two printing mistakes:

(i) the units of H (the conduction-convection heat transfer parameter per unit area of sphere), as quoted in the footnote on p 65 should be
(cal sec^{-1} deg C^{-1} mm^{-2}); and

(ii) equation (15) - as used on p 68 - should have read:

$$K = 1.2\pi a\,(Sc)^{1/3}\,(Re)^{1/2}\,L_v D. \qquad (15)$$

Scientific Reports and Technical Notes of the Present Series

MW-1: Effect of particle shape and secondary scattering on microwave reflections from clouds and precipitation, by Milton Kerker and Walter Hitschfeld, March 1951.

MW-2: Measurement of snow parameters by microwaves, by J.S. Marshall and K.L.S. Gunn, May 1951.

MW-3: The modification of rain with distance fallen, by E. Caroline Rigby and J.S. Marshall, January 1952.

MW-4: Interpretation of the fluctuating echo from randomly distributed scatterers: Part I, by J.S Marshall and Walter Hitschfeld, October 1951.

MW-5: Scattering and absorption of microwaves by a melting ice sphere, by M.P. Langleben and K.L.S. Gunn, March 1952.

MW-6: Interpretation of the fluctuating echo from randomly distributed scatterers: Part II, by P.R. Wallace, December 1951.

MW-7: The microwave properties of precipitation particles, by J.S. Marshall, T.W.R. East and K.L.S. Gunn, July 1952.

MW-8: Precipitation trajectories and patterns, by J.S. Marshall, M.P. Langleben and E. Caroline Rigby, August 1952.

MW-9: A theory of snow crystal habit and growth, by J.S. Marshall and M.P. Langleben, July 1953.

MW-10: The modification of rain in showers with time, by E. Caroline Rigby, and J.S. Marshall, March 1953.

MW-11: A mathematical treatment of random coalescence, by Z.A. Melzak and Walter Hitschfeld, March 1953.

MW-12: Errors inherent in radar measurement of rainfall at attenuating wavelengths, by Walter Hitschfeld and Jack Bordan, June 1953.

MW-13: Radar evidence of a generating level for snow, by K.L.S. Gunn, M.P. Langleben, A.S. Dennis and B.A. Power, July 1953.

MW-14: Initiation of showers in cumuli by snow, by A.S. Dennis, July 1953.

MW-15: Turbulence in clouds as a factor in precipitation, by T.W.R. East and J.S. Marshall, July 1953.

MW-16: The terminal velocity of snow aggregates, by M.P. Langleben, January 1954.

MW-17: Development during fall of raindrop size distributions, by E. Caroline Rigby, K.L.S. Gunn and Walter Hitschfeld, January 1954.

MW-18: The effect of wind shear on falling precipitation, by K.L.S. Gunn and J.S. Marshall, December 1954.

MW-19: The convection associated with release of latent heat of sublimation, by R.H. Douglas and J.S. Marshall, December 1954.

MW-20: A: Size distribution generated by a random process, by Walter Hitschfeld. B: The distribution with size of aggregate snowflakes, by K.L.S. Gunn and J.S. Marshall, September 1956.

MW-21: Pattern in the vertical of snow generation, by R.H. Douglas, K.L.S. Gunn and J.S. Marshall, July 1956.

MW-22: Precipitation mechanisms in convective clouds, by T.W.R. East, January 1956.

MW-23: Measurement and calculation of fluctuations in radar echoes from snow, by Walter Hitschfeld and A.S. Dennis, July 1956.

MW-24: The plan pattern of snow echoes at the generating level, by M.P. Langleben, February 1956.

MW-25: A possible role of hail in formation of tornadoes, by Walter Hitschfeld and J.S. Marshall, March 1957.

MW-26: Growth of precipitation elements by sublimation and accretion, by R.H. Douglas, May 1957.

MW-27: Studies of Alberta hail storms 1957, by R.H. Douglas and Walter Hitschfeld, May 1958.

MW-28: Electronic constant altitude plan position indicator for a weather radar, by T.W.R. East, November 1958.

MW-29: The motion and erosion of convective storms in severe vertical wind shear, by Walter Hitschfeld, July 1959.

MW-30: Alberta hail, 1958, and related studies. Parts I and II by R.H. Douglas, Part III by R.H.D. Barklie and N.R. Gokhale, July 1959.

MW-31: The quantitative display of radar weather patterns on a scale of grey, by T.H. Legg, June 1960.

MW-32: Weather-radar attenuation estimates from raingauge statistics, by P.M. Hamilton and J.S. Marshall, January 1961.

MW-33: Improvements in weather-radar grey scale, by F.T. Barath, July 1961.

MW-34: Interim account of hail studies - November 1960, by R.H. Douglas, J.S. Marshall and R.H. D. Barklie, Reprinted in April 1962.

MW-35: Alberta Hail Studies, 1961, by A.E. Carte, R.H. Douglas, C. East, K.L.S. Gunn, Walter Hitschfeld, J.S. Marshall, E.J. Stansbury, December 1961.

MW-36: Alberta Hail Studies, 1962/1963, by A.E. Carte, R.H. Douglas, R.C. Srivastava and G.N. Williams, August 1963.

MW-37: Precipitation profiles for the total radar coverage, by P.M. Hamilton, September 1964.

MW-38: Two studies of convection, by R.C. Srivastava and C.D. Henry, October 1964.

MW-39: Interpretation of the fluctuating echo from randomly distributed scatters: Part 3, by Paul L. Smith, Jr., December 1964.

MW-40: Facsimile and areal integration for weather radar, Vols. I and II, by Marceli Wein, April 1965.

MW-41: Time-dependent characteristics of the heteorogeneous nucleation of ice, by Gabor Vali and E.J. Stansbury, April 1965.

MW-42: Alberta Hail Studies, 1964, by J. Derome, R.H. Douglas, Walter Hitschfeld, M. Stauder, July 1965.

MW-43: Attenuation of a parallel beam of light, particularly by snow, by Olav Lillesaeter, April 1965.

MW-44: Measurements on new fallen snow, by K.L.S. Gunn, August 1965.

MW-45: Measurements on falling snow, by K.L.S. Gunn and M. Wein.

MW-46: Experiments on the nucleation of ice, 1961-63, by G. Vali and E.J. Stansbury, August 1965.

MW-47: Studies of the formation of precipitation in convection by R.C. Srivastava and M. English, August 1966.

MW-48: Part I of Air Transport Association Report "Parameters for Airborne Weather Radar" by J.S. Marshall, C.D. Holtz and Marianne Weiss, December 1965.

MW-49: Alberta Hail Studies, 1966, by A.J. Chisholm, Marianne English, Walter Hitschfeld, Jerry Pell, N.H. Thyer, May 1967.

The following reports of the MW series are related specifically to hail studies:

MW-27, May 1958. Studies of Alberta hailstorms 1957. R.H. Douglas and Walter Hitschfeld.

MW-30, July 1959. Alberta hail, 1958, and related studies.
Alberta field studies. R.H. Douglas.
Growth by accretion in the ice phase. R.H. Douglas.
The freezing of supercooled water drops. R.H.D. Barklie and N.R. Gokhale.

MW-34, November 1960. Interim account of hail studies.
Interim account of Alberta hail studies. R.H. Douglas and J.S. Marshall.
Size distributions, ice contents and radar reflectivities of hail in Alberta. R.H. Douglas.
Radar observations of Alberta hailstorms. R.H. Douglas.
Inter-relation of the fall speed of rain and the updraft rates in hail formation. J.S. Marshall.
Heterogeneous nucleation is a stochastic process. J.S. Marshall.
Nucleation measurements on rain and melted hail. R.H.D. Barklie.

MW-35, December 1961. Alberta hail studies, 1961.
The study of an Alberta hailstorm. R.H. Douglas.
A theory of hail growth. Walter Hitschfeld and R.H. Douglas.
Radar reflectivities of hail samples. R.H. Douglas.
The Stormy Weather Group's five-dimensional weather radar. J.S. Marshall and K.L.S. Gunn.
Stochastic freezing. E.J. Stansbury.
Hailstone measurements and structure. A.E. Carte.
Grain growth in ice. A.E. Carte.
A technique for analyzing meso-scale pressure patterns. C. East, S.J.
Hail research around the world. Walter Hitschfeld.

MW-36, August 1963. Alberta hail studies, 1962/1963.
Some characteristics of Alberta hailstorms. A.E. Carte.
Continuity of hail production in Alberta storms. G.N. Williams and R.H. Douglas.
Size distributions of Alberta hail samples. R.H. Douglas.
Entrainment in cumulus: a review. R.C. Srivastava.

MW-38, October 1964. Two studies of convection.
A model of convection with entrainment and precipitation. R.C. Srivastava.
High radar echoes from Alberta thunderstorms. C.D. Henry.

MW-41, April 1965. Time-dependent characteristics of the heterogeneous nucleation of ice. Gabor Vali and E.J. Stansbury.

MW-42, July 1965. Alberta hail studies, 1964.
Large-scale vertical motion and the occurrence of severe storms. J.F. Derome.
Size distributions of Alberta hail samples. R.H. Douglas.
The temperature of hailstones. W. Hitschfeld and M. Stauder.
A postscript to Report MW-38.

MW-46, August 1965. Experiments on the nucleation of ice 1961-63.
E.J. Stansbury and G. Vali.

MW-47, August 1966. Studies of the formation of precipitation in convection.
The effect of precipitation on cumulus dynamics. R.C. Srivastava.
A new program for the calculation of hail growth. M. English.

MW-49, May 1967. Alberta hail studies, 1966.
A new method of double theodolite pibal evaluation. N.H. Thyer.
Continuity in hail production and swaths. J. Pell.
Small scale radar structure of Alberta hailstorms. A.J. Chisholm.
On the temperature of hailstones. M. English and W. Hitschfeld.

Technical Notes

MWT-1: Photography at the AN/CPS-9 weather radar at Montreal Airport, by M.P. Langleben and Walter Hitschfeld, January 1955.

MWT-2: The elevation controller for CAPPI operation of the AN/CPS-9 weather radar, by T.W.R. East. Submitted under Contract No. AF19(604)-1579, October 1956.

MWT-3: An optical system for automatic synthesis of constant-altitude radar maps, by M.P. Langleben and W. Denis Gaherty, January 1957.

MWT-4: On the measurement of cloud temperatures from the ground by infra-red radiation, by Walter Hitschfeld, October 1960.

BLANK PAGE

unclassified

Security Classification

DOCUMENT CONTROL DATA - R&D

(Security classification of title, body of abstract and indexing annotation must be entered when the overall report is classified)

1. ORIGINATING ACTIVITY *(Corporate author)*
McGill University
Stormy Weather Group
Montreal 2, Canada

2a. REPORT SECURITY CLASSIFICATION
Unclassified

2b. GROUP

3. REPORT TITLE
ALBERTA HAIL STUDIES 1966

4. DESCRIPTIVE NOTES *(Type of report and inclusive dates)*
Scientific. Interim.

5. AUTHOR(S) *(Last name, first name, initial)*
A.J. Chisholm
Marianne English
Walter Hitschfeld
J. Pell
N.H. Thyer

6. REPORT DATE
May 1967

7a. TOTAL NO. OF PAGES
81

7b. NO. OF REFS
32

8a. CONTRACT OR GRANT NO.
F19628-67-C-0129

b. PROJECT, Task, Work Unit Nos.
8620-04-01

c. DoD Element 6144501F

d. DoD Subelement 671310

9a. ORIGINATOR'S REPORT NUMBER(S)
MW-49
Scientific Report No. 2

9b. OTHER REPORT NO(S) *(Any other numbers that may be assigned this report)*
AFCRL-67-0657

10. AVAILABILITY/LIMITATION NOTICES
1- Distribution of this document is unlimited. It may be released to the Clearinghouse, Department of Commerce, for sale to the general public.

11. SUPPLEMENTARY NOTES
TECH, OTHER

12. SPONSORING MILITARY ACTIVITY
Air Force Cambridge Research Laboratories (CRH)
L.G. Hanscom Field
Bedford, Massachusetts 01730

13. ABSTRACT

Thyer: A new method is presented for evaluating double theodolite pibals, using all four theodolite angles to locate the most likely position of the balloon. The calculation may be done graphically, once a special chart has been compiled, so straightforward calculations of wind are possible without use of a computer.
Pell: Although some storms may generate hail continuously, in the manner of the Wokingham storm of Browning and Ludlam, there are cases of storms which produce intermittent hailswaths disrupted by patches of only rain. Closely related to the problem of swath continuity is that of continuity of hailfall at a point. Again, reports have been recorded which indicate that frequently hail falls in "bursts" separated by periods of either rain or no precipitation at all.
Chisholm: A study of radar echo maxima in two Alberta hailstorms has shown that the storms consisted of several storm "families", each containing small intense radar echo "cores" or cells. These cells developed preferentially on the right flank of the family, moving across the track of the family at an acute angle to dissipate near the left flank; identifiable lifetimes of the cells were 20-30 minutes. There appeared to be a cycle of development of the cells, which had a considerable effect on the overall storm-family velocity.

DD FORM 1 JAN 64 1473

unclassified

Security Classification

unclassified

Security Classification

14. KEY WORDS	LINK A		LINK B		LINK C	
	ROLE	WT	ROLE	WT	ROLE	WT
Hailstorms Radar meteorology Storm motions Pibal calculations Hail intermittency						

INSTRUCTIONS

1. ORIGINATING ACTIVITY: Enter the name and address of the contractor, subcontractor, grantee, Department of Defense activity or other organization *(corporate author)* issuing the report.

2a. REPORT SECURITY CLASSIFICATION: Enter the overall security classification of the report. Indicate whether "Restricted Data" is included. Marking is to be in accordance with appropriate security regulations.

2b. GROUP: Automatic downgrading is specified in DoD Directive 5200.10 and Armed Forces Industrial Manual. Enter the group number. Also, when applicable, show that optional markings have been used for Group 3 and Group 4 as authorized.

3. REPORT TITLE: Enter the complete report title in all capital letters. Titles in all cases should be unclassified. If a meaningful title cannot be selected without classification, show title classification in all capitals in parenthesis immediately following the title.

4. DESCRIPTIVE NOTES: If appropriate, enter the type of report, e.g., interim, progress, summary, annual, or final. Give the inclusive dates when a specific reporting period is covered.

5. AUTHOR(S): Enter the name(s) of author(s) as shown on or in the report. Enter last name, first name, middle initial. If military, show rank and branch of service. The name of the principal author is an absolute minimum requirement.

6. REPORT DATE: Enter the date of the report as day, month, year, or month, year. If more than one date appears on the report, use date of publication.

7a. TOTAL NUMBER OF PAGES: The total page count should follow normal pagination procedures, i.e., enter the number of pages containing information.

7b. NUMBER OF REFERENCES: Enter the total number of references cited in the report.

8a. CONTRACT OR GRANT NUMBER: If appropriate, enter the applicable number of the contract or grant under which the report was written.

8b, 8c, & 8d. PROJECT NUMBER: Enter the appropriate military department identification, such as project number, subproject number, system numbers, task number, etc.

9a. ORIGINATOR'S REPORT NUMBER(S): Enter the official report number by which the document will be identified and controlled by the originating activity. This number must be unique to this report.

9b. OTHER REPORT NUMBER(S): If the report has been assigned any other report numbers *(either by the originator or by the sponsor)*, also enter this number(s).

10. AVAILABILITY/LIMITATION NOTICES: Enter any limitations on further dissemination of the report, other than those imposed by security classification, using standard statements such as:

(1) "Qualified requesters may obtain copies of this report from DDC."

(2) "Foreign announcement and dissemination of this report by DDC is not authorized."

(3) "U. S. Government agencies may obtain copies of this report directly from DDC. Other qualified DDC users shall request through

_____."

(4) "U. S. military agencies may obtain copies of this report directly from DDC. Other qualified users shall request through

_____."

(5) "All distribution of this report is controlled. Qualified DDC users shall request through

_____."

If the report has been furnished to the Office of Technical Services, Department of Commerce, for sale to the public, indicate this fact and enter the price, if known.

11. SUPPLEMENTARY NOTES: Use for additional explanatory notes.

12. SPONSORING MILITARY ACTIVITY: Enter the name of the departmental project office or laboratory sponsoring *(paying for)* the research and development. Include address.

13. ABSTRACT: Enter an abstract giving a brief and factual summary of the document indicative of the report, even though it may also appear elsewhere in the body of the technical report. If additional space is required, a continuation sheet shall be attached.

It is highly desirable that the abstract of classified reports be unclassified. Each paragraph of the abstract shall end with an indication of the military security classification of the information in the paragraph, represented as *(TS), (S), (C), or (U).*

There is no limitation on the length of the abstract. However, the suggested length is from 150 to 225 words.

14. KEY WORDS: Key words are technically meaningful terms or short phrases that characterize a report and may be used as index entries for cataloging the report. Key words must be selected so that no security classification is required. Identifiers, such as equipment model designation, trade name, military project code name, geographic location, may be used as key words but will be followed by an indication of technical context. The assignment of links, rules, and weights is optional.

unclassified

Security Classification